Republic of Iraq
Ministry of Higher Education and Scientific Research
University of Babylon
College of Materials Engineering
Department of Ceramics Engineering and Building Materials

The Magnetic behavior of Nickel Ferrite/Barium Ferrite system

A Thesis
Submitted to the Council of the College of Materials Engineering/University of Babylon in Partial Fulfillment of the
Requirements for the Master degree in Materials Engineering/ Ceramic

By:
Amany Hatem Shaker Mahdi

Supervised by:
Dr. Shaima'a J. Kareem
Dr. Mohammed N. Al-Aaraji

2023 A.D
1443 A.H

بسم الله الرحمن الرحيم

﴿قَالُوا سُبْحَانَكَ لَا عِلْمَ لَنَا إِلَّا مَا عَلَّمْتَنَا إِنَّكَ أَنْتَ الْعَلِيمُ الْحَكِيمُ﴾

صدق الله العلي العظيم

سورة البقرة – ايه (32)

Supervisor Certification

I certify that this thesis entitled (The Magnetic behavior of Nickel Ferrite/Barium Ferrite system) had been carried out under my supervision at the University of Babylon/College of Materials Engineering/ Department of ceramic engineering and building Materials in partial fulfillment of the requirements for the degree of Master in Material's Engineering/Ceramic.

Signature:

*Name :**Assist. Prof. Shaima' a J. Kareem (PhD)***

(Supervisor)

Date: / / 2023

Signature:

*Name: **Lecture. Mohammed Naji (PhD)***

(Co-Supervisor)

Date: / / 2023

Signature:
Dr. Prof. Mohsin Abbas Aswad (Ph. D)

Head of Ceramics Engineering and Building Materials

Date: / / 2023

(Examination Committee Certification)

We certify that we had read this thesis entitled **(**The Magnetic behavior of Nickel Ferrite/Barium Ferrite system**)** and as an Examination Committee, we examined the student (***Amany Hatem Shaker*****)** in its contents and that in our opinion it meets the standard of a thesis and is adequate for the award of the Degree of Master in Materials Engineering/ Ceramic.

Signature
Prof. Imad A. Disher (PhD)
Date: / /2023
(Chairman)

Signature
Prof. Niveen Jamal(phD)
Date: / / 2023
(Member)

Signature
Assist.Prof. Kutaiba Al-Marzoki(PhD)
Date: / / 2023
(Member)

Signature:
Assist.Prof. Shaima' a J. Kareem(PhD)
University of Babylon
Date: / / 2023
(Supervisor)

Signature:
Lecture. Mohammed Naji(phD)
University of Babylon
Date: / / 2023
(Co-Supervisor)

Signature:
Prof. Mohsin Abbas Aswad (PhD)
Date: / / 2023

Signature:
prof. Imad A. Disher (phD)
Date: / / 2023

Dedication

To my family, friends, and anyone who inspired me.

Acknowledgments

First of all, profusely all thanks be for **Allah** lord of all creations who enabled me to achieve this work.

I would like to express my deep thanks to the college of Materials Engineering/ University of Babylon for giving me the chance to complete my study.

I would like to express my deep gratitude and appreciation to my supervisor **Dr. Shaima'a Jaber. Kareem and Dr. Mohammed Naji Al-Aaraji** for their advice, support and encouragement that they gave me during the course of work. Their suggestions and moral support in difficult times have been essential for completing this work. I am very proud to achieve my work under their supervision.

I want to express my appreciation and gratitude to the head of department, **Prof. Mohsin Abbas Aswad (PhD)**, all academic staff, and support staff in the ceramics department.

My deep appreciation goes to the support staff of ceramic materials laboratories, for their help.

I would also like to thank all my friends and colleagues during the study in the college, for creating an unforgettable environment in which my research was carried out.

Abstract

Due to its composition, ceramic magnets are sometimes referred to as ferrite magnets. They are made up of several metallic elements and iron oxide. These substances combine to form the magnetic compound known as ferrite. Simply said, hard ferrite magnets have a high coercivity and soft ferrite magnets have a low coercivity. Soft ferrite magnets with low coercivity are more likely to get demagnetized when exposed to an external magnetic field.

In this work, $NiFe_2O_4$ and $BaFe_2O_4$ soft/hard composites and soft/hard/soft layers were prepared. Nickel ferrite spinel ($NiFe_2O_4$) is one of the most well-known soft ferrites, and hard ferrite (barium ferrite) needle-like of hard ferrite with special properties were both synthesized by sol-gel method using hydrated nickel nitrate , barium nitrate, hydrated iron nitrate and ethylene glycol as a solvent where using 2: 1 weight ratio of iron nitrate hydrated to barium nitrate and nickel nitrate ,after preparing powder was calcined for five hours at a rate of 5 °C/min at 600 °C for nickel ferrite and 800 °C for barium ferrite to being acquired as a dry powder.

In the present work, there are two main parts , the first part is formation pure materials of soft(nickel), hard (barium) ferrites and composite with a different proportions , the second part includes preparing the bulk material as a pure , composite materials and in the form of layers . The XRD test was performed for the pure and composite materials of soft and hard ferrites shown the main peaks of nickel ferrites ($NiFe_2O_4$), barium ferrite with different phases at different temperatures and for composite the peaks of two materials nickel and barium ferrite according their ratio . The FTIR spectrum obtained from the synthesized material show the main bands of nickel ferrite higher one (v1) in the range of 630-550 cm-1, lowest band (v2) found in the range 450-390 cm-1 , barium ferrite Peaks at 1147 cm-.1, 1058 cm-.1, and 1001 cm-1 and their composite high-

frequency band between 570 and 610 cm-1 . From the images of the SEM test, the shape of the nanoparticles of nickel ferrite showed the spherical shape and contained porosity where the image of barium ferrite show the needle-like shape . VSM test shown a different magnetization Ms , different hysteresis loops the S shape of soft nickel ferrite with a high magnetic saturation and super paramagnetic properties , high corctivity for a hard ferrite(2593.479Oe) , single smooth hysteresis loop for a nanocompo site and layers of hard/soft ferrites. where the tests done after sintering .the highest Ms finding in a soft ferrite is (39.586) and in layers is equal to (37.589) and the highest Hc was in hard ferrite and in sample with 75% barium ferrite .where increasing in corcivity and magnetic saturations depend on the ratio of soft and hard ferrites.

In addition, doing the XRD test, FTIR and VSM of the nickel ferrite , barium ferrite and composite ferrite ,density , porosity and shrinkage tests were performed after ferrites sintering, where observed porosity in a sintering samples and a little shrinkage occurred after sintering process.

Table of Contents

1 Introduction and Objectives.....1

1.1 Introduction 1

1.2 Aims of the study: 4

2 Background and Literature review 5

2.1 Magnetic Materials.....5

2.2 Types of Magnetic Material.....6

2.3 Ferrite 8

2.4 Classification of Ferrites 9

2.4.1 According to Magnetic Properties: 10

2.4.2 Based on Crystal Structure.....15

2.5 composite hard /soft ferrites.....20

2.6 Methods of Preparation of Ferrite 22

2.6.1 The sol gel Method 22

2.7 Literature Review.....26

3 Experimental procedures 36

3.1 Materials and Chemicals. 36

3.2 Preparation Ferrite Powders.....39

3.2.1 Preparation Nickel Ferrite (Soft) 39

3.2.2 Preparation barium Ferrite(hard) 41

3.3 Composite particles hard –soft ferrites.....43

3.4 preparation of bulk samples 44

3.4.1 Preparation pellets ferrite 44
3.5 Morphological and Microstructure Characterization 45
3.5.1 X-ray diffraction Analysis 46
3.5.2 Scanning Electron Microscopy (SEM) Analysis 46
3.5.3 FT-IR Analysis 47
3.6 Magnetic Characterizations: 47
3.6.1 Vibrating Samples Magnometer (VSM) Measurement: 47
3.7 Physical Characterization of ferrite 48
4 Results and Discussion 51
4.1 Structural Characterization 51
4.1.1 X-Ray Diffraction Analysis. 51
4.1.2 Scanning Electron Microscope (SEM) analysis 56
4.1.3 FT-IR analysis. 62
4.2 Magnetic Characterizations: 66
Physical Characterization of Ferrite 72
5 Conclusion and Recommendation 79
5.1 Conclusion 79
5.2 Recommendation 80
6 References 81

List of Figures

Figure 2-1 Different types of magnetic behavior [20]. 8
Figure 2-2 Phase diagram of the Ba-Fe-O system [47]. 14
Figure 2-3 Size and form of the hysteresis loops for hard and soft magnets are compared [48]. 14
Figure 2-4 (a) cell structure of the spinal unit, (b) Interstice in octahedron (32 per unit cell at B site; 16 occupied), (c) Interstice tetrahedral (A location: 64 cells per unit, 8 occupied) [57]. 17
Figure 2-5 Unit Cell of barium ferrite, $BaFe_{12}O_{19}$ [15] 19
Figure 2-6 Steps of the sole gel processing of materials and examples of the microstructure of final products[87]. 26
Figure 3-1 Flowchart illustrates the steps and stage of work 38
Figure 3-2 Flowchart Illustrate the Steps to Prepare nickel ferrite powder.....40
Figure 3-3 Flowchart Illustrate the Steps to Prepare Barium ferrite powder. 42
Figure 3-4 Ferrite layers.....44
Figure 4-1 XRD analysis forNickelsamplesat 800°Cand 1200°C.....52
Figure 4-2 XRD analysis for composite ferrite samples at 800°C 54
Figure 4-3 XRD analysis for composite ferrite samples at 1200°C ..... ….55
Figure 4-4 XRD analysis for Barium ferrite samples at 800°C and 1200°C.....56
Figure 4-5 SEM images: a- NiFe2O4 at 600 °C, b- NiFe2O4 at 1200 °C 57
Figure 4-6images SEM : a- nano composite with ratio 50/50 at 800 °C, b- nano composite with ratio 50/50 at 1200 °C C – nano composite with ratio 75/25 nickel ferrite / barium ferrite at 1200 °C d - nano composite with ratio 25/75 nickel ferrite / barium ferrite at 1200 °C 59
Figure 4-7 SEM images: a- $BaFe_2O_4$ at 800 °C, b- $BaFe_2O_4$ at 1200 °C 60
Figure 4-8 SEM images: a- Barium ferrite layer at 1200 °C, b- Nickel ferrite layer at 1200 °C.....61

Figure 4-9 a- FTIR OF $NiFe_2O_4$ at 600 °C, b-FTIR OF $NiFe_2O_4$ at 1200 °C 63
Figure 4-10 FTIR oF Barium ferrite at 1200 °C.....64
Figure 4-11 FT -IR spectrum composite nickel/barium with ratio 50/50 ferrites at 1200 °C 65
Figure 4-12 hysteresis loop of soft ferrite 66
Figure 4-13 a- hysteresis loops soft(nickel) /hard(barium) with 25% Ba sintering at 1200°C b- hysteresis loops soft(nickel) /hard(barium) with 50% Ba sintering at 1200°C c- hysteresis loops soft(nickel) /hard(barium) with 75% Ba sintering at 1200°C 68
Figure 4-14 hysteresis loop developed for the barium ferrite 69
Figure 4-15 showed hysteresis loop developed for the layers soft/hard/soft ferrites 70
Figure 4-16 a- Hysteresis loops at 1200 °C temperature for nickel ferrite ,composite ferrite , barium ferrite and layers b- Ms, Mr for ferrite samples c- coricivity (Hc) for ferrite samples.....71

List of Tables

Table 2-1 Summery of literatures in Hard-Soft ferrite graded 33
Table 3-1 Substances, Chemical Formula, Purity, Source, and the phase state of the Chemicals for start material. 36
Table 3-2 materials and forms of prepared samples 45
Table 4-1 particles size of samples at 600°C and 1200°C.....61
Table 4-2 Magnetic properties of Ferrites Samples.....72
Table 4-3 Physical Characterization 73

List of Abbreviations

Abbreviation	Name
NPs	Nanoparticles
M_S	Saturation Magnetization
Hc	Coercivity
FTIR	Fourier Transform Infrared
SEM	Scanning Electron Microscopy
VSM	Vibrating Sample Magnometer
XRD	X-Ray Diffraction
(BH)max	Maximum energy product
(M)	Magnetization
(H)	applied field
RF	Radio frequency
MNPs	magnetic nanoparticles
FCC	face-centered cubic
dw	domain wall width
UV	Ultraviolet
BF	Barium Ferrite
NF	Nickel Ferrite
SFNS	Spinal Ferrite Nanoparticles
AM	Amplitude Modulation
NCS	Nanocomposites

List of units

Units Used	Meaning
nm	nanometer
Å	angstrom
ºC	degree Celsius
min	minute
Cm^{-1}	reciprocal centimeter
g/cm^3	gram/ cubic centimeter
ml	milliliters
MHz	Megahertz
GHz	Gigahertz
mm	millimeter
g	gram

Chapter One

1 Introduction and Objectives

1.1 Introduction

This category encompasses every aspect of life that include magnetic fields and their impact on substances. Magnetic fields can be produced by magnets or electric currents on a macroscopic scale.

However, a fundamental ideas and mechanisms that underlie the magnetic phenomena are intricate and delicate, and until very recently, physicists were unable to fully grasp them. Today's technological advances depend heavily on magnetic and magnetism materials, electric engines, generator and transformer of electric power, telephones, radio, television, computers, as well as other components of sound and picture reproduction systems are a few examples.

The naturally occurring mineral lodestone, different steels, and iron are well-known examples of magnetic materials that exhibit magnetic properties.

The following are crucial details concerning magnetic materials:

1. Some materials have magnetic properties even in the absence of a magnetic field, and they become significantly more magnetic in the presence of a low magnetism.

2. A number of materials that, when heated over optimum temperature, lose their initially high magnetism and instead become very weakly magnetic.

3. A few materials exhibit a magnetic response with any external applied field.

4. Magnetic substances can be magnetized in a magnetic field, or they can generate their own magnetic field [1].

All magnetic materials may be divided into two categories from the perspective of applications:

(i) hard magnet materials.

(ii) soft magnet materials[1] .

Magnetic nanocomposites and layers of soft and hard ferrite fabricated due to its numerous uses in permanent magnet have garnered a lot of attention[2,3]. Kneller et al [4]In the early 1990s, it was proposed that nano composite magnets include both soft- and hard-magnetic substances.

Research on hard/soft ferrite nano composites has seen a significant increase in attention due to significant advancements in the exchange spring idea. Because they are inexpensive, environmentally safe, and there is a large supply of iron oxide in nature, ferrites in nanostructure have become significant materials in both commercial and industrial applications [5].

There are two primary categories of ferrites: soft spinel ferrites and hard ferrites. Soft ferrites have a cubic structure and characterized by resonance frequency in the megahertz region, high saturation, high chemical oxidation resistance, high magnetic permeability, and low coercivitys. Hard ferrites, which constitute the second kind, have a high coercivity, a substantial energy production, with a frequency in the gigahertz range and reduced magnetic saturation. It is difficult to obtain a magnetic material that possesses high coercive force and residual magnetism so research has increased to obtain a new material with unique magnetic properties was produced by combining soft and hard ferrites. These innovative materials have a greater surface area, a wider absorption spectrum, as seen by high magnetic energy product (BH)max values with saturation magnetization Ms. These properties make them very appealing for a variety of applications.

Across the layer at the exchange length, which equates to a domain wall width, spins switch from the soft layer to the hard layer at the interfacial layer. The two-phase magnetic system acts like a single-phase magnet in this case because the magnetic reversal takes place at the system's coercive field. Due to the fact that the interface may be appropriately built using bilayers, this well-defined process is more likely to occur there than in bulk nanocomposites. The interfacial features in bulk nanocomposites are influenced by things such as degree of atomic coherence, chemical and atomic affinity etc [6].

1.2 Aims of the study:

The main aim of this work was to study the influence of combine soft and hard ferrites in different forms on structure, microstructure and magnetic properties of the resulted products. With supposing, that the resulted functionally graded ferrites can be exhibited better characteristics in comparison with constituent ferrites, where the soft ferrite phases having a greater magnetic moment and the hard ferrite phases having a larger coercively.

To attain this object, the work was conducted in the following stages:

1. Preparation of nickel and barium ferrites by using a sol-gel method as represented of soft and hard ferrite, respectively in pure form.
2. Utilize of sol-gel method to prepare a powder as composite of soft and hard ferrites in different percentage, where (Soft:hard) weight ratio were; (75:25), (50:50) and (25:75).
3. Preparation of bulk samples throughout pressing in different form, as pure, composite and in the form of layers (soft:hard:soft).
4. In this study, a sol-gel technique was used. Through using low-cost tools and being straightforward to make, for producing fine and uniform soft/hard ferrite powders

Chapter Two

2 Background and Literature review

Material in the present era of research and technology, science and engineering is crucial. The dramatic growth as well as expansion throughout the post-World War II era, electrical ceramics era have been contributed significantly to the shift in civilization from the Steel Age to the Information Age. Without concurrent breakthroughs in semiconductors, dielectrics, ferroelectrics, ferrites, and optoelectronics, practically instant county to country satellites telecommunications and from across entire world it wouldn't conceivable. modifications in superconducting ceramics, photonics, and optical waveguides, as well as perhaps in optical computing and information processing, have paralleled and may eventually surpass the ongoing discoveries in these domains [7]. Magnetic ceramics have been studied in relation to developments in communication technologies because of their incredibly exciting characteristics, including magnetic patterns, substantial magnetic conductivity, and high electrical resistivity [8]. They are without a doubt the most adaptable technical high frequency uses for ceramics, such as energy converters, antenna elements, faraday rotators, etc. due to these inherent material features [9].

2.1 Magnetic Materials

Magnetite (Fe_3O_4), the earliest magnetic substance known to man, is where the history of magnetism begins. Although its early history is hazy, its ability to draw iron was undoubtedly recognized 2500 years ago. Magnetite is found in many places. The territory of Magnesia in what is now modern Turkey was home to the most abundant deposits in antiquity, and the term "magnet" is derived from a closely related Greek word that is thought to have originated from the name of this region [10]. Based on their magnetic characteristics, magnetic materials may be roughly divided into five primary categories. They are ferromagnetic , antiferromagnetic,

ferromagnetic, paramagnetic, and diamagnetic. Their magnetic susceptibility (χ) can also be used to differentiate them as they respond differently to an applied magnetic field. Diamagnetism is the property of materials with no permanent magnetic moments, paramagnetic is the property of materials with magnetic moments that do not interact with one another, and ferromagnetism, anti-ferromagnetism, or ferrimagnetism is the property of materials with strong interactions between the magnetic moments [11] . The term "magnetic materials" refers to a broad category of materials with a wide range of uses. Electricity is produced, distributed, and for the most part used in appliances by the usage of magnetic materials. They are employed to store data on computer disks as well as audio and video tapes. They are utilized in body scanners and a variety of medical applications where they are affixed to or implanted within the body [12].

2.2 Types of Magnetic Material

Magnetic materials are divided in to five groups namely

a-Diamagnetic Materials

The atoms in a diamagnetic material have no magnetic moment when there is no applied field. The spinning electrons precess when an applied field (H) is present, and this form of electric current motion results in magnetization (M) that goes against the direction of the applied field [13].

b- Paramagnetic Materials

Magnetic moments produced by unpaired electrons inside the material give rise to paramagnetism. The magnetic moments are only slightly aligned when an

applied magnetic field, because of which there is a low magnetization in the same direction as the applied field [14].

c-Ferromagnetic Materials

Only a small number of metals, particularly Fe, Co, Ni, and Ni, additionally several rare earth minerals atoms (and ions) that exhibit strong magnetic effects that lead to economically significant materials[15]. ferromagnetic materials even in the absence of a magnetic field, exhibit high magnetization because of the simultaneous aligns of magnetization. Compared to paramagnetic materials, ferromagnetic materials are far more susceptible, saturable at extreme temperatures and mild magnetic fields [16].

d- Antiferromagnetic Materials

Chromium is the one element in the periodic table to have antiferromagnetism at ambient temperature. Contrary to ferromagnetic materials, antiferromagnetic materials have their atomic magnetic properties aligned in an antiparallel direction as a result of the exchange interaction between nearby atoms [17]. CoO, NiO, and FeO are a few examples of known antiferromagnetic substances [18].

e-Ferrimagnetic Materials

A ferrimagnetic substance is one that, like an antiferromagnetic substance, includes populations of atoms with opposing magnetic moments, however these moments are not of the same magnitude, leaving room for spontaneous magnetization [19]. This types of magnetic can be shown in figure (2.1).

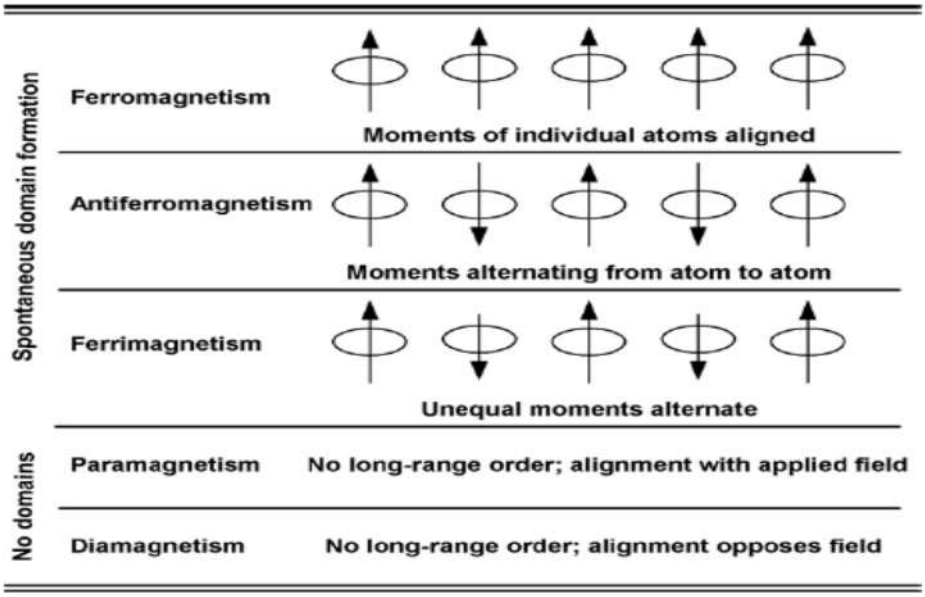

Figure 2-1 Different types of magnetic behavior [20].

2.3 Ferrite

One magnetic oxide compound called ferrite has iron oxide as its main constituent. Ferrites are composed of quick transition metals, such as iron, chromium, and manganese, as well as lanthanides compounds. The Zn^{+2}substituted Ni and Mn ferrite, also known as $NiZnFe_2O_4$ and $MnZnFe_2O_4$, respectively, are the most significant commercially viable variants of these ferrites [21].Ferrites have a dark brown or gray color and an extremely brittle physical makeup. The different transition metal oxides or alkaline earth oxides are heated with the ferric oxides to prepare them. Ferrite exhibits ferrimagnetisms as a result of super-exchange interaction between metal electrons and oxygen ions[22]. The features of ferrites such as high resistance, broad frequency spectrum (10 kHz to 50 MHz), affordable, a variety of materials ,adaptability of form ,cost-effective assembly and stability of temperature and time.

The usage of ferrite has increased as a result of its unique properties like high permeability, time/temperature stability, wide-band transformers, tunable inductors, delay lines, and other high-frequency electronic circuitry. Ferrites are commonly used in high-frequency applications as other circuit components' high frequency performance keeps improving. incorporated into magnetic circuits for both low-level and high-power applications [23]. Despite ferrite has a lower saturation magnetization than ferromagnetic alloys, they offer stronger heat resistance and corrosion resistance [24]. The majority of ferrites lack electrical conductivity, which makes them beneficial for uses like reducing eddy currents in magnetic materials for transformer. This is in contrast to other ferromagnetic materials [25]. Ferrites additionally did in a computer wire as a lump, renowned as a bead of ferrite, which aids in preventing the egress of high-frequency electric sound (radio wave interference) or trying to enter the device [26]. Due to their distinct physical, magnetic, and chemical characteristics that set them apart from their bulk counterparts, nanoparticles ferrite nanostructures have garnered a lot of attention in recent years. Most frequently, they are utilized in magnetic-based applications like magnets, medication delivery, memory storage, etc. As a result of their unique electrochemical characteristics, such as their ability to exist in a variety of redox states, their electrochemical stability, and their mechanical toughness, nano crystalline ferrites are being investigated as prospective electrode materials for energy storage devices[27].

2.4 Classification of Ferrites

Ferrites are classified depending on their crystal structure and magnetic properties. Ferrites come in two different varieties: soft ferrite and hard ferrite.

2.4.1 According to Magnetic Properties:

Depending on whether their magnetic has a low or high coercivity, ferrites are classified as "soft" or "hard" materials [28].

2.4.1.1 *Soft ferrites*

High Ms and low Hc are important attributes for soft ferrites. Soft ferrites have small hysteresis loops as a result [28]. Compounds containing nickel, zinc, or manganese are found in ferrite nanoparticles that are utilized as electromagnetic or transformer cores[29]. Permanent magnets are not found in soft ferrites. They are magnetic (similar to mild steel), but their magnetism reduces after removal of the magnetic force. Transformers frequently employ soft ferrite (to transform the primary's voltage secondary windings). The outcome is, transformer ferrite is another name for soft ferrites. They are not very coercive. The magnetism of the substance may fast alter direction without employing a lot of energy thanks to its low coercivity (hysteresis losses), the hysteresis loop of soft ferrite can be seen in figure (2.3). . Owing to their comparatively low loss at higher frequency, these have frequently employed in the cores of RF inductors and transformers as purposes for switched-mode power supplies and loopstick antennas used in AM radios.

The soft ferrites that are most frequently encountered are $Ni_xZn_{(1-x)}Fe_2O_4$, commonly known as nickel-zinc ferrite (NiZn), NiZn ferrites are better suited for frequencies over 1 MHz due to their higher resistivity than MnZn ferrites [30].

NiZn ferrites are commonly utilized above 5 Megahertz, whereas Below that frequency, MnZn ferrites are employed extensively. The common mode inductors are an exception, and their chosen threshold is 70 MHz [31].

A-Nickel ferrite

Owing to its typical characteristics, decreased eddy current losses due to poor conductivity, good stable electrochemistry, catalytic activity, nature is abundant, ect. One of the useful and important softer ferrites for technology is nickel ferrite [32]. This ferrite is an inverted spinel in which each unit cell of the spinel structure contains eight units of $NiFe_2O_4$. Tetrahedral sites (A-sites) are preferentially occupied by half of the ferric ions, whereas octahedral sites (B-sites) are home to the remaining ferric ions [33]. Consequently, the formula may be used to represent the compound (Fe^{+3}) A [$Ni^{+2}Fe^{+3}$] BO_4 [34]. Recently, there have been a lot of research done on the synthesis of spinel ferrite nanoparticles, and it has been highlighted how the preparation conditions primarily affect the morphological and structural characteristics of the ferrites [35]. NiFe2O4 ferrites, also known as Spinel ferrites have a low electrical conductivity along with a number of attractive magnetic properties. They have reduced eddy current loss in alternating current applications, unlike magnetic metals, alloys, and especially helpful in the band of radio frequencies. Because of this, spinel ferrites are frequently utilized in recording heads, as well as in the cores of various transformers, inductors, and TV deflection devices, as well as in recording tapes. The kind of ions, their charges, and how they are distributed throughout the tetrahedral (A) and octahedral (B) sites determine the remarkable electrical and magnetic characteristics of ferrites [36].

The cubic face-centered lattice of $NiFe_2O_4$ exhibits a completely inverted spinel structure. The typical formula of this mixed metal oxide is AB_2O_4. In $NiFe_2O_4$, Fe^{+3} ions occupy the tetrahedral (A) sites whereas Ni^{+2} andFe^{+3}ions are equally distributed across the octahedral (B) sites [37]. A meticulous and cautious approach has always been necessary to create $NiFe_2O_4$ ceramic with optimal

characteristics. Essential factors including density, grain size, and porosity must be under control in order to enhance electrical and magnetic characteristics. Prior to now, grain growth by sintering and densification optimization have been used to enhance the magnetic and electrical characteristics [38].

2.4.1.2 ***Hard Ferrite***

Hard ferrites, on the other hand, which after magnetization have a strong remanence and a high coercivity, are used to create permanent ferrite magnetics. Hard ferrite magnetic made by using iron oxide, barium or strontium carbonate [39] [40]. Due to their high coercivity, the materials are particularly resists demagnetization. The hysteresis loop of hard ferrite can be seen in figure (2.3).

It is essential for the a permanent magnet. Additionally, they have a significant magnetic permeability. These allegedly ceramic magnets cheap and often utilized in household products like refrigerator magnets [41].

B-Barium Ferrite

One of the most often utilized magnetic materials is barium hexaferrite. Nowadays hexaferrite of barium ($BaFe_{12}O_{19}$), which is hexagonal in structure, is frequently employed in microwave equipment, magnetic recording medium, and permanent magnets . Ferrites and garnets are examples of ferromagnetic oxides that have magnetic and dielectric properties. Compared to other permanent magnets like NdFeB, SmCo which are ideal for a variety of radio frequency (RF) and microwave applications, the ferromagnetict usually has lesser energy . Magnetoplumbite (M-type) is the structure, and its usual formula is ($MFe_{12}O_{19}$) or $M_{0.6}Fe_2O_3$, where M could be lead, strontium, or barium (Pb) [42]. Hard magnetic material made of barium hex ferrite ($BaFe_{12}O_{19}$-magnetoplumbite structure) has a

large saturation magnetization, a high Curie temperature, and good chemical stability. Barium hex ferrite can be made in a variety of ways, microstructures and processing methods have a big impact on the material's magnetic characteristics [43]. The $BaFe_{12}O_{19}$ barium hex ferrite is corrosion resistant and has excellent chemical stability, making it suitable for use essentially without end and safe for the environment. Permanent magnets with adequate specific magnetic energy can be produced by combining a strong coercive force with a high enough residual induction [44]. This fact prompted significant efforts to substitute various cations or cation combinations into barium hex ferrite to change its magnetic properties, either exclusively on the iron site or concurrently on the iron and barium sites. It is essential for substituted ions in all such modified ferrites to keep electrical neutrality and share the same ionic radii as the original one [45].Figure (2.2) shows the phase diagram of BF at different Temp and compositions

Barium monoferrite ($BaFe_2O_4$) is best known as an intermediate phase created during the synthesis of the technologically significant barium hexaferrites. It can exist in either a spinel or an orthorhombic phase [46].

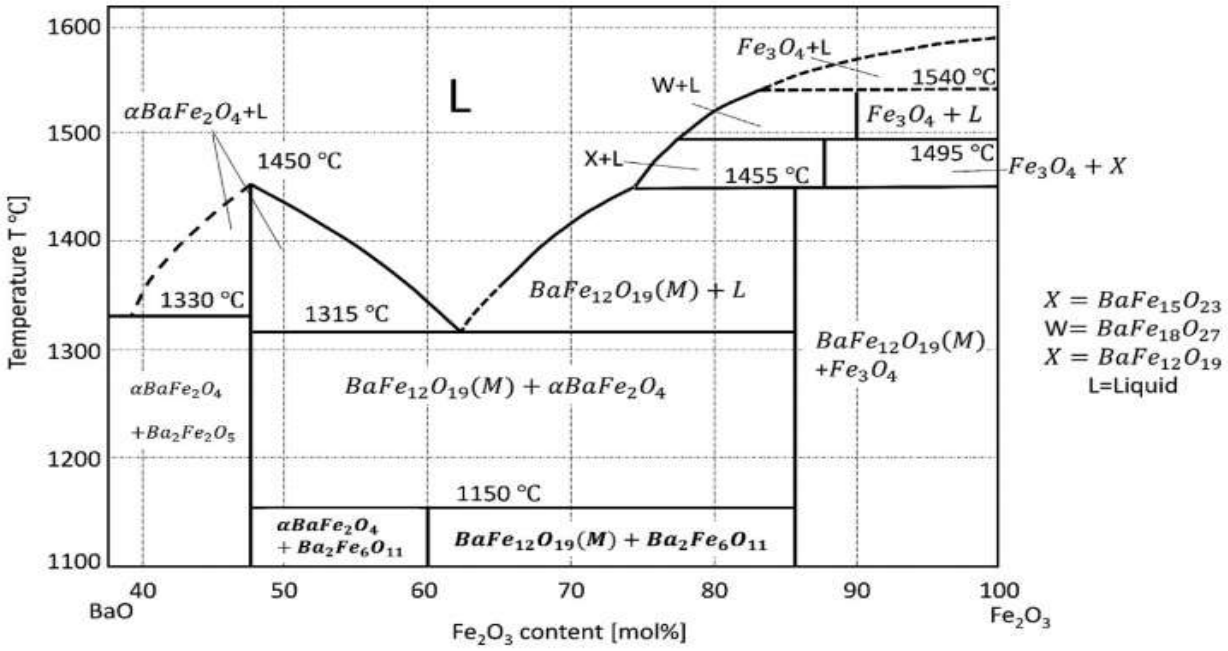

Figure 2-2 Phase diagram of the Ba-Fe-O system [47].

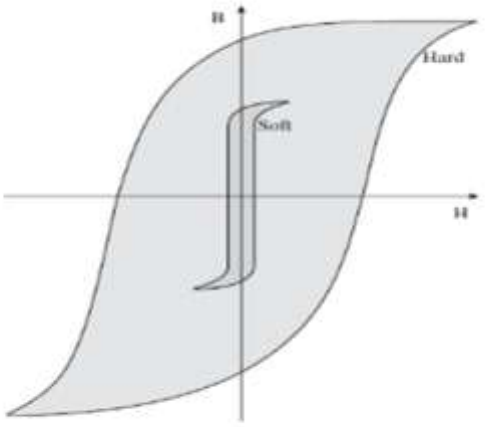

Figure 2-3 Size and form of the hysteresis loops for hard and soft magnets are compared [48].

2.4.1.3 ***Semi hard ferrite***

Between soft and hard magnetic materials, CoFe2O4 (CoO•Fe2O3) is a semi-hard magnetic combination [49], is made of cobalt. The majority of its uses are in magnetostrictive devices such as sensors and actuator. because of its high saturation magnetostriction (200 ppm)[50]. $CoFe_2O_4$ is a good alternative to Terfenol-D because it offers the benefit of not requiring rare earths [51]. The magneto electric effect in composite is also improved by the induced magnetic anisotropy in cobalt ferrite [52].

2.4.2 Based on Crystal Structure

The eventual use is typically connected to the crystal structure. For instance, BaO and Fe_2O_3 combine to generate a hexagon structure, that have features a unique crystal axis that lends self-assisted permanent magnetic. The cubic crystal structure , on the other hand provides a significant number of similar crystal orientations and also be useful in situations when avoiding a preferred direction is preferable [15] .Based on their crystal formations, ferrites may be divided into three categories hexagonal ferrites, garnet ferrites, and spinel ferrites [53].

I-Spinel

A wide group of ferrites with this structure. In a perfect spinel structure, oxygen atoms are arranged in a cubic close-packed (FCC) array. Anions, with cations occupying one-eighth of the tetrahedral (A) sites and one-half of the octahedral (B) sites. Eight AB_2O_4 formula units make up one unit cell, which has 32 octahedral sites and 64 tetrahedral sites [54] . structure of spinal unite with octahedral and tetrahedral sites show in figure (2-4) .For some minerals of the spinel group, including spinel itself, $MgAl_2O_4$, the space group is really the tetrahedral F43m, not the Fd3m . Owing to Ferrites spinel's have good biocompatibility,

minimal toxicity, and magnetism (AFe_2O_4), A is a transition metal that is divalent, for example Fe ,Ni, Zn , Cr, Mn, or Co.) have gained a lot of attention in recent years due to their distinctive features and potential uses as catalysts, gas sensors, rechargeable batteries, and high-density data storage. spinel ferrite nanoparticles (SFNs) have attracted a lot of attention in contemporary basic science. Lithium batteries, data storage devices, magnetic bulk cores, magnetic fluids, microwave absorbers, medical diagnostics, and therapeutic procedures are a few examples[55]. Therefore, from both a practical and theoretical standpoint, it is essential to understand the structural and magnetic characteristics of spinel's. The distribution cation and/or structural characteristics of these properties may be changed by altering the synthesis techniques, annealing temperature or applying the doping suitable elements to the B-site or A-site.

A face-centered cubic (FCC) structure of ferrite spinel is made up of a closely packed cubic oxygen lattice. 32 oxygen atoms make up a spinel ferrite's unit cell, 8 divalent metal ions (M), and 16 trivalent iron ions. Two interstitial positions in the spinel structure are filled by metal cations that have oxygen coordinated octahedra (B) and tetrahedra (A) [55, 56].

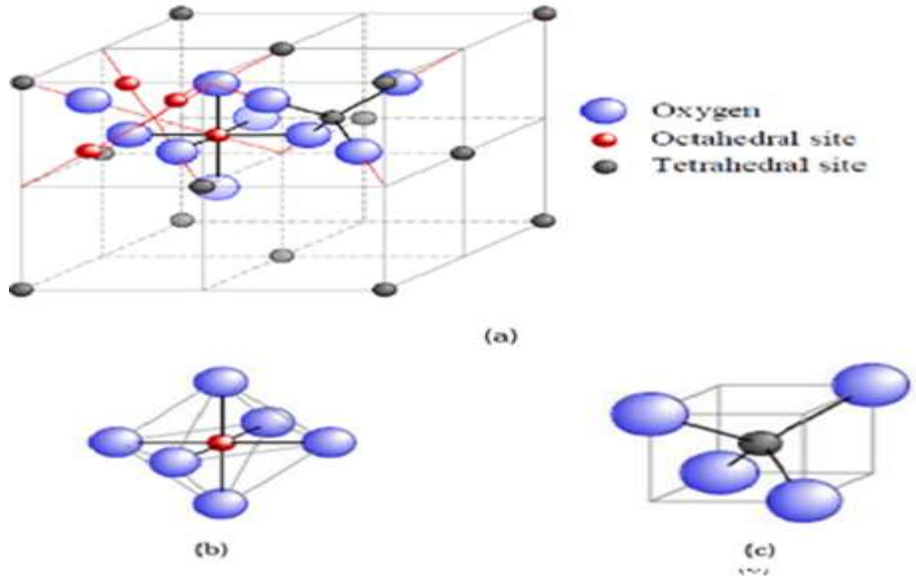

Figure 2-4 (a) cell structure of the spinal unit, (b) Interstice in octahedron (32 per unit cell at B site; 16 occupied), (c) Interstice tetrahedral (A location: 64 cells per unit, 8 occupied) [57].

I-1 Normal spinel's

Eight tetrahedral and sixteen octahedral sites, or each formula unit has one tetrahedral site and two octahedral sites, are occupied by metal ions in a spinel lattice unit cell. Each formula unit has four octahedral sites and eight tetrahedral sites are typically found in cubic close-packed oxides, which make up normal spinel structures. In comparison to octahedral spaces, tetrahedral spaces are smaller. While A ions fill one-eighth of the tetrahedral holes, B ions occupy half of the octahedral holes. The mineral spinel $MgAl_2O_4$ has structure a normal spinel [58].

I-2 Inverse Spinel's

Inverse spinel's are spinel's with particular structure, Take nickel ferrite, for example, that has 8 units of $NiFe_2O_4$ in each spinel unit cell. Only half of the ferric ions can fit in the available space in the tetrahedral positions (eight). The remaining eight, together with the eight Ni^{+2}ions, are placed on the octahedral sites. Antiparallel to the eight Fe(+3)moments on the tetrahedral sites are these eight $Fe^{(+3)}$moments and eight Nickel moments. While the magnetic or uncompensated moment is produced by the ions of nickel at certain moments, the moments on the Fe^{+3}ion moments simply cancel. An inverted ferrite is the name given to this kind of ferrite. Numerous crucial ferrites for commerce are inverted [15] . According to the values often found in the corresponding bulk spinels, X-ray absorption fine structure shows that the degree of spinel structural inversion rises in the series Mn, Co, and Ni spinel. where the degree of inversion in $NiFe_2O_4$ ferrites is 1.00. $NiFe_2O_4$ is a totally inverted spinel structure with all nickel ions in the octahedral sites (i = 1) [59].

II-Hexagonal ferrites

The magnetoplumbite crystal structure has hexagonal symmetry as opposite to the spinel crystal structure's cubic symmetry. It therefore has a large preferred axis called the c axis, as well as a minor axis called the a axis. Utilizing the desired directionsas a permanent magnet material has benefits. Like with the spinel structure, Ions of oxygen are closely packed, but there are layers of oxygen that now contain Sr^{+2},Ba^{+2} or Pb^{+2} ions. This might potentially replace the oxygen ions in the lattice since their ionic radii are relatively similar. Figure(2.5) show the schematic structure of the hexa-ferrite $BaFe_{12}O_{19}$. contains several layers overall, among which two have the Ba^{+2} four layers, each with four ions oxygen. followed by layer containing one Ba^{+2}ion and three oxygen ions , follows a layer of three oxygen ions

and one Ba^{+2} ion that is located in the opposite Ba"" ion in the layer that contained Ba^{+2}, there are four further levels with four oxygen ions each. These 10 layers' interstices are home to all the Fe^{+3}ions. In addition to the tetrahedral and octahedral locations, One more type of site, where a trigonal bi-pyramid is formed by the metal ion surrounded by five oxygen ions is also present, but is absent from the spinel structure [15].

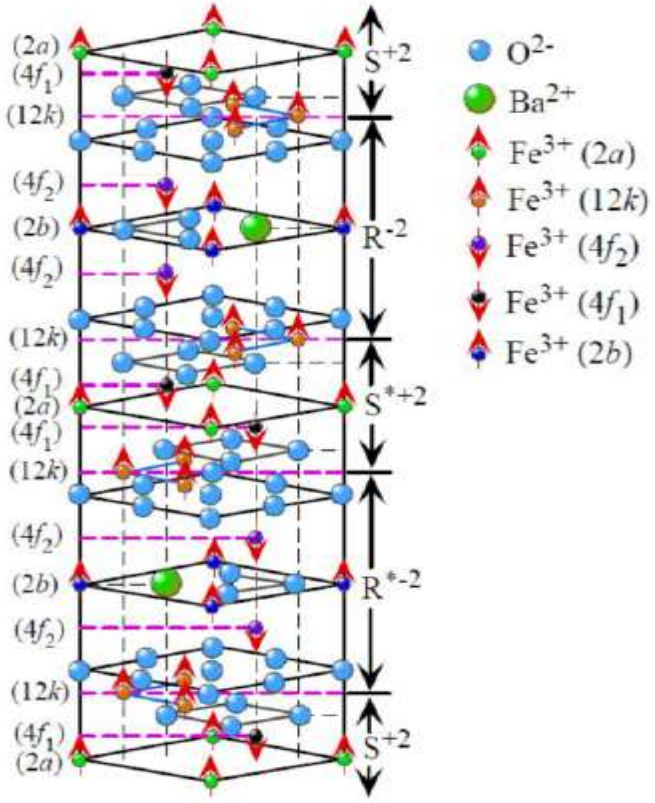

Figure 2-5 the schematic structure of the hexa-ferrite $BaFe_{12}O_{19}$ [15].

III-Garnets

Garnet have a 12-sided or dodecahedral crystal structure similar to that of the garnet stone. The general $3M_2O_3.5Fe_2O_3$. In contrast to the other two classes, the

metal ions in this instance are all trivalent ,M is commonly yttrium(Y) or another rare earth ion in magnetic garnets [15].

IV-Orthoferrites

The perovskite or 6orthoferrite structure next most significant structure after garnets, hexagonal ferrites, and spinel's. MFeO3 is the formula, M typically refers to yttrium or a rare earth. Rather than being cubic, the structure is orthorhombic. Anti-ferromagnetic ally canting or non-parallel alignment of coupled ions is what causes the weak ferromagnetism [15].

2.5 composite hard /soft ferrites

The increased capabilities of composite materials that have a precise blend of hard and soft magnetic phases make them candidates for a range of possible applications as permanent magnets [60]. The two phase magnetic nano composites' magnetic behavior is significantly influenced by the exchange and dipolar interactions and even the size, distribution, and shape of the grains. Obtaining high coercivity (Hc) and high saturation of magnetization (Ms) concurrently is a significant difficulty for magnetic materials. As a result, by combining hard and soft phases create composite materials resulted from various attempts to reconcile this issue [60]. Whereas the phase of hard magnetism introduces strong coercivity, High saturation magnetization is produced by soft phase. Additional research confirmed the extensive homogenous mixing for the creation of exchange spring magnets, the hard and soft ferrite layers have to be balanced [61,62].One of the critical objectives of contemporary applied physics is the creation of novel functional composites with adjustable magnetic and microwave characteristics. Scientists currently interested in functional hard-soft magnetic composites; In a number of sectors, such as catalysis, major contributions have been made by spinel ferrites and composites based on them

[63,64], microwave, gas sensors [65], magneto-optical data storage [66], targeted medicine delivery [67], cancer therapy, telecommunications, photoactive materials, and catalysts are some examples of related technologies. One of the most appealing applications for complex iron oxides is microwave absorption, which has great saturation magnetization (Ms), high coercively (Hc), and significant interaction between magnetic phases [68,69] . due to its high coercively (Hc), high saturation magnetization (Ms), magnetic phases exhibit strong interaction. This presents fresh opportunities for the use of magnetic materials in electronics[70]. Due to their affordability, Ferrite composites composed of hard ferrites and spinel soft are desirable candidates for enhanced permanent magnets because of their higher resistance to corrosion, comparatively high Curie temperature, and high electrical resistivity [71]. The two phases of the hard/soft ferrite composites have an excellent exchange spring interaction, such hard/soft composites are $CoFe_2O_4$/CoFe,$SrFe_{12}O_{19}$/$Ni_{0.5}Zn_{0.5}Fe_2O_4$, $BaFe_{12}O_{19}$/$NiFe_2O_4$, $BaCa_2Fe_{16}O_{27}$/Fe_3O_4, $Ni_{0.8}Zn_{0.2}Fe_2O_4$, and $SrFe_{12}O_{19}$/$NiFe_2O_4$ [72] .When the high HC from the hard material and the high MS from the soft material are combined into one material (nano composite), the exchange spring magnets, the product (BH)max is significantly increased compared to any one of the nano composite's component phases [73].

Despite the exchange spring behavior's theoretical foundations have been empirically achieved in bulk for a number of systems [74,75] . Both inherent magnetic qualities and microstructural characteristics influence magnetic characteristics of magnetic substances. As a result, important variables include things like grain boundary type, grain size, and particle shape, along with these features, the distribution of magnetic hard and soft phases controls how magnetic properties of composites behave[76]. In metallic systems, A great deal of research

has been done on the exchange spring behavior. However, More study is needed on the concept of exchange coupling between soft and hard phases in the context of an oxide nano composite permanent magnet [77].

2.6 Methods of Preparation of Ferrite

To create ferrites with best properties, purity, stability, and surface area, manufacturing processes are crucial. The chemical synthesis techniques provide rapid and efficient approaches to produce nanocrystals. They frequently provide the benefits like broadened scope and enhanced capabilities, enabling the synthesis of all possible kinds of nanoparticles Currently, a number of synthesis methods are being used to create ferrite materials, each of which has advantages and disadvantages of its own. Top-down and bottom-up strategies are the two main types of synthesis techniques. The components are ground into tiny particles for a "top-down" course, whereas in ions are chemically mixed in a "bottom-up" process to create the particles. Thermal decomposition, hydrothermal, solvothermal, sol-gel, microwave-assisted, vapor deposition, micro emulsion, polyol, flame spray pyrolysis, coprecipitation , etc. are examples of "bottom-up" synthesis techniques, while under a "top-down" techniques are pulsed laser ablation and mechanical milling [78].

2.6.1 The sol gel Method

A wet-chemical method called the sol-gel process is utilized to create ceramic and glassy materials. In this procedure, the sol progressively develops into a network that consists of a gel-like liquid phase and a solid phase. Metal alkoxides and metal chlorides are typical precursors that are transformed into a colloid by poly condensation and hydrolysis processes. The underlying morphology or structure of

the solid phase might be anything from continuous polymer networks that resemble chains to discrete colloidal particles [79][80].

A more chemical (wet chemical) way for creating different nanoparticles, metal oxide nanoparticles, in particular, is a sol-gel method . Low temperatures and a liquid state are employed in the sol-gel procedure. Naturally, the final result is a solid, and throughout a polymerization process, which entails joining the metal atoms in the raw materials to produce M-OH-M or M-O-M bonds (where M stands for the metal atom), solids are produced.

A sol-gel procedure consists of the following two phases.

1. The production of distinct, colloidal solid particles of nano scale diameters occurs in the first step.

2. Colloidal particles combine in the solvent during the second phase to form a gel

The sol-gel method is used to create synthesis from the bottom up. The final products of this process are the consequence of several irreversible chemical reactions. Procedures create a three-dimensional version of the initial homogeneous molecules (sol), endless, heavy molecule known as a gel [81].

The sol-gel process is a practical one, and the products' chemical composition may be well controlled thanks to the low processing temperatures.

Materials created by a sol-gel technique used in several optically, electric, surface engineering, energy, biosensor, medical, and separations techniques. The creation

of a homogenous sol from the precursors and its transformation into a gel are basic steps of a sol gel process. figure (2-6) shown the steps of the sole gel process.

Once the solvent has been eliminated from the gel's structure, the residual gel is dried. The features of the dried gel are significantly influenced by the drying method. In other words, the "removing solvent approach" is selected in accordance with how the gel will be used. Additionally, 99.99% pure composites with a high degree of homogeneity may be created using sol-gel process. Another advantage this technique has over traditional methods is the reduced process is temperature, which makes it possible to create metal and ceramic nanomaterial at temperatures between 70 and 320°C [81].The most advantages of sol –gel Process is creation of products with high purity , extremely high production efficiency, capability to design and manage chemical composition in order to achieve a homogenous composition, the capacity to create composite oxides from homogenous compounds[82].

PH, temperature, water/alkoxide ratio, metal alkoxide activity, and solution conditions, the kind of solvent employed, and the additive utilized are some of the factors influencing the hydrolysis and condensation processes (sol-gel process). Using catalysts often to control the volume and speed of condensation and hydrolysis processes is another factor to take into account. These processing parameters can be changed to create materials with various surface chemistries and microstructures [83]. A sol-gel method's chemical procedure involves dispersing a processed materials in solvent first, then a hydro process happens to produce the activated monomers. Before forming into a gel with a certain spatial arrangement, the active monomer starts to polymerize and change into a gel. Nanoparticles and the necessary ingredients are produced after drying and heat treatment [84].

The Sol gel method's fundamental reaction stages are listed below [85]:

1-Solvation: The solvent unit, $M(H2O)n^{(+z)}$, is formed when the metal cation M(+Z) attracts water molecules. It has a strong propensity to leak H+ to keep its coordination number.

$M(OR)n^{+2} \rightarrow$ M(H2O)n_1(OH)z_1 $+H^{+}$

2- Hydrolysis process: Water reacts with precursor molecules such as metal alkoxide M(OR)n that are non-ionizing.

M(OR)n+ xH2O→M(OR)n_x(OH)x

M(OR)n-x(OH)x+ x ROH→ M(OH)n

3) Reactions of poly condensation: It may be classified into two groups based on the types of molecules eliminated.

a) Poly condensation of dehydration

-M-OH + HO-M→-M-O-M- + H2O

b) The poly condensation of deal coholization

-M-OR + HO-M→-M-O-M- + ROH

sol-gel process may be applied quickly since the raw components are first dispersed into a solvent to create a low-viscosity solution. We achieve uniformity at the molecular level. The reactants are probably evenly mixed at the molecular level while creating a gel. The chemical reaction will be simpler to carry out than

the solid-phase reaction and just necessitate lower temperature synthesis. It a commonly accepted that the sol-gel system's component diffusion occurs at nanometer scales. Although solid phases reaction's component diffusion is in the micrometer range, a reaction is still straightforward conduct since the temperature is low, and by choosing the right circumstances, many new materials may be made [86].

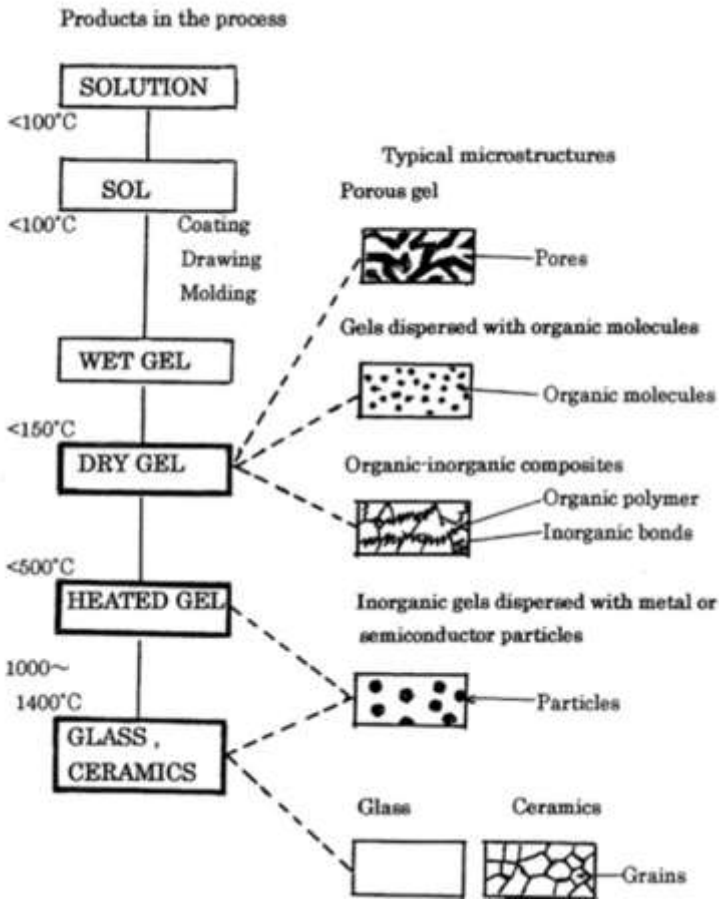

Figure 2-5 Steps of the sole gel processing of materials and examples of the microstructure of final products[87].

2.7 Literature Review

One of the key objectives of contemporary applied physics is the creation of novel functional composites with adjustable magnetic and microwave characteristics. In reality the presence of magnetically soft and hard phases, the average grain sizes of

the different phases, the shape of the particles, etc, all greatly affect the magnetic characteristics of two-phase nano composite materials. Modern scientists are interested in useful hard-soft magnetic composites, some summery scientists show in table (2-1) . The prediction of a single hard-phase magnetic behavior for a nano composite composed of both soft- and hard-magnetic phases is made possible by high exchange coupling between the two distinct phases .This is referred to as the behavior of the exchange spring, which is very helpful in creating better permanent magnets. therefore, scientists have developed new methods for integrating hard-soft ferrite materials .

Teh, et al, in (2007). Used sol-gel process for preparation and investigations of Co (II) and Co (III)-substituted barium ferrite . This approach was made in an effort to increase the end product's homogenization. The sol-gel method was used to create $BaM_XFe_{12}XO_{19}$ [M = Co(II) or Co(III), and X = 1.0]. The precursor employed was ethylene glycol, and mass of, $Fe(NO_3)3•9H_2O$, $Ba(NO_3)2$,$Co(NO_3)2•6H_2O$, acetylacetonate (98%) or cobalt (III) were dissolved at 50 C for two hours . The samples obtained were reasonably homogeneous and the average particle size obtained via the chosen synthetic route (using ethylene glycol as gel precursor) was confirmed to be in the nano-sized range [88].

Paimozd , et al, in (2008). Study the effect of acid catalysts on the magnetic and structural characteristics of Nano crystalline barium ferrite synthesized via sol-gel. By using sol-gel methods, $BaFe_{12}O_{19}$ powders nano crystalline size were created. The magnetic characteristics were enhanced stearic, hydrochloric, nitric, and acetic acids are used. In this study, aqueous sol was created by combining Iron nitrate with barium nitrate ($Ba(NO_3)2$) , (Fe/Ba = 10.5). To improve the nitrate dissolution, ethanol was added to the sol [89].

Rai, et al, in (2014). Study the synthesis and magnetic properties of hard-soft $SrFe_{10}A_{l2}O_{19}/NiZnFe_2O_4$ ferrite nano-composites. $SrFe_{10}A_{l2}O_{19}$ (soft) NiO. 75ZnO. $25Fe_2O_4$ were prepared via auto combustion method, A linear increase in Mr/Ms with soft-phase content indicates the presence of enhanced exchange-coupling between hard and soft phases. This simple method seems to be a promising way to tailor and enhance the magnetic properties of oxide based hard-soft magnetic nanocomposites [90].

Neupane, et al, in (2017). Synthesis and study the magnetic properties of magnetically hard-soft $SrFe_{12-y}AlyO_{19-x}$ Wt.% Ni0. 5ZnO. $5Fe_2O_4$ nano composites. SrFe12-yAlyO19/Ni0.5Zn0.5Fe2O4 exchange coupled magnetic nano composites were effectively synthesized by one-pot auto combustion. High Ms was attained at y=0.0 and 50 Wt.% $Ni_{0.5}Zn_{0.5}Fe_2O_4$, while the composite's best Ms (73.5 emu/g) and Hc (4330 Oe) values were found at y = 1.0 and 20 Wt.% $Ni_{0.5}Zn_{0.5}Fe_2O_4$ content. These numbers outperform the magnetic characteristics of pure $SrFe_{12}O_{19}$. Additionally, it was found that the composite's Curie temperature increased as its soft phase content rose[91].

Khan, A. A., et al, in (2017). Investigate nanocrystalline $NiFe_2O_4$ particles that prepared by conventional sol-gel, citrate-nitrate sol-gel combustion and coprecipitatio methods. Investigations into the structural, chemical, morphological, optical, and magnetic characteristics of nickel ferrite were conducted after the produced samples were annealed at 1000 °C for two hours. We have succeeded in synthesizing nickel ferrite nanoparticles by sol-gel wet chemical, sol-gel auto-combustion and co-precipitation methods. The sol-gel derived sample showed higher purity compared to the other two, the smaller value of MS compared to the bulk value in the prepared samples was attributed to the greater fraction of surface spins in these nanoparticles [92].

Tavakolinia, et al ,in (2018). Studied improved exchange coupling in novel hard/soft ferrite composite particles and magnetic characteristics in ceramics processing and application. $SrFe_{12}O_{19}/Zn_{0.4}Co_{0.2}Ni_{0.4}Fe_2O_4$ to make hard/soft ferrite composite particles with 20, 40, 60, and 80 weight percent's of soft phase, one-pot sol-gel auto-combustion and physical mixing procedures were used. The hard/soft ferrite composite particles exhibited good exchange coupling between hard and soft ferrite phases in the samples prepared by physical mixing and one-pot methods and possessed high saturation magnetization and The coercivity of the samples is reduced by increasing soft phase amount [93].

Peymanfar, et al, in (2018). synthesized $BaFe_2O_4$ spinel structures through the sol–gel method using a low sintering temperature, investigation of $BaFe_2O_4$ nanoparticles' microwave absorption characteristics at Ku-band frequency using silicone rubber medium and sol-gel route for their production and identification. The results show the use of the sol-gel method and a low sintering temperature to create $BaFe_2O_4$ nanoparticles, proving that the nanoparticles' crystal purity was significantly impacted by the heat treatment. According to the XRD patterns, phase impurities of nanoparticles disappeared when the temperature increased, the results suggest that $BaFe_2O_4$ nanoparticles can be a promising microwave absorbing material [94].

Hussain, S. A.in (2019, July). Review the structure and magnetic properties of Co^{+2}–Ti^{+4} substituted barium ferrite powder prepared by sol–gel method. Throughout this study, the Sol-gel technique is used to make Co^{+2}-Ti^{+4} substituted barium hex ferrite particles as well as hexagonal barium ferrites. As the beginning materials, an appropriate amount of barium nitrate ($Ba(NO_3)2$), iron nitrate ($Fe(NO_3)3$), and citric acid ($C_6H_8O_7.H_2O$) were dissolved in distilled water. The results show that the products calcenid at 950^oC for 5 h at a rate of 150 ^oC/h. to

obtain a ferrite powder, the particles of all the samples exhibit plate-like shape and they have different granular sizes with a clear agglomerate in severalvery large clusters [95].

Kahnes & Töpfer, in (2019). They synthesis and study the magnetic properties of hard/soft $SrA_{l2}Fe_{10}O_{19}$/Fe ($FeCo_2$) nano composites. Hard/soft magnetic nanocomposites were synthesized with $SrA_{l2}Fe_{10}O_9$ as hard and $CoFe_2$ or Fe as soft magnetic Phase. A mixture of hexaferrite and nanosize $CoFe_2O_4$ particles was annealed at 315 °C in $Ar/_{5\%}H2$ atmosphere. The spinel ferrite particles were reduced to $CoFe_2$ alloy. Alternatively, soft iron nanoparticles were deposited onto the Al-substituted hexaferrite particles via a sodium borohydride reaction. The results presented here on the morphology, phase formation and magnetic response of hexaferrite/Fe($FeCo_2$) nanocomposites do not point at the existence of strong exchange coupling [96].

Algarou et al in (2020). Enhance the exchange coupling behavior of $SrCo_{0.\ 02}Zr_{0.\ 02}Fe_{11.\ 96}O_{19}/MFe_2O_4$ (M= Co, Ni, Cu, Mn and Zn) as hard/soft magnetic nano composites. Using a one-pot sol-gel combustion method, hard/soft $SrCo_{0.02}Zr_{0.02}Fe_{11.96}O_{19}/MFe_2O_4$ (M=Ni, Co, Cu, Mn, and Zn) nano composites have been successfully created[97].

Lee, et al, in (2020). The hard/soft magnetic fibers were simply prepared via a bottom-up approach, combining an electrospinning process and calcium-assisted reduction. Direct in-situ chemical synthesis, which does not involve any complicated procedures or equipment, was effective in producing composition-controllable hard/soft magnetic nanofibers or instruments. Only the precursor solution used for electro spinning's chemical composition was under control. Extra pure Sm was utilized as the first reagent $(NO_3)\ 3{\bullet}6H_2O$, $Co(NO_3)\ (NO_3)\ 2{\bullet}6H_2O$,

$Fe(NO_3)$ (NO_3) Citric acid, poly vinyl pyrolidone (PVP; Mw 1,300,000), and $3•9H_2O$[98].

Irfan, & Vizhi, in (2020). improve the energy product at its maximum for Co-precipitated of $Y_3Fe_5O_{12}/Ba_{0.5}Sr_{0.5}Fe_{12}O_{19}$ nano-composite. A two-step co-precipitation approach was used to create the Nano composite ferrite made of $Ba0.5Sr_{0.5}Fe_{12}O_{19}$ and Y3Fe5O12 with soft (YIG) and hard (BSFO) magnetic phases. In the nano composite ferrites $(1\text{-}y)Ba_{0.5}Sr_{0.5}Fe_{12}O_{19}/(y)Y_3Fe_5O_{12}$, Various ratios of the soft magnetic phase addition were used (x = 0.1, 0.0, 0.3, 0.2, 0.4, and 1) to produce the ferrites. Without any secondary phase, the hard and soft phases' presence has been confirmed by XRD analysis showing the ferrite nano composite's production. For (0.9)BSFO/(0.1)YIG, Coercivity and magnetization have improved, as shown by the magnetic data. The optimized (0.1)YIG \(0.9)BSFO nano composite demonstrated a 57% increase in energy product (BH)max compared to pure BSFO, indicating the nano composite's superior exchange coupling. In this work, co-precipitation approach is used to create exchange coupled cubic yttrium iron garnet and low anisotropy hexagonal barium strontium ferrite with significant c-axis anisotropy and high magnetic field in various ratio. These two phases working together can enhance the materials' magnetic properties [99].

Almessiere, et al, in(2021). Found that nano composites of hard-soft $Sr_{0.5}Ba_{0.5}Eu0.01Fe_{12}O_{19}/NixCuyZnwFe_2O_4$ exhibit changes in their magnetic and electrodynamics characteristics. The S1- $Ni_xCu_yZn_wFe_2O_4$ S5 $Sr_{0.5}Ba_{0.5}Eu_{0.01}Fe_{12}O_{19}$ NCs were produced using a one-pot sol-gel auto-combustion process. Both hard and soft phases, with crystal sizes ranging from 20 to 85 nm, were produced, per the XRD data. Hexaferrite and spinel ferrite were found to co-

occur as an aggregate consisting of a hexagonal plate covered by a cluster of cubic particles, according to the surface analysis [100].

Almessiere ,et al, in (2021). Review the functional bi-component nano composites based on hard/soft ferrites: Structural, magnetic, electrical and microwave absorption property . One important strategy to do this is by combining materials with various properties to create new function materials (, bilayer, core-shell etc.). This study's primary objective is to provide a summary of connections between magnetic, microwave, dielectric, and exchange-coupled characteristics of hard/soft (spinel) ferrites nano composites and their consequences on microstructure [101].

Slimani, et al, In (2021), study the relationship between composition, magnetically, optically, and microwave characteristics in the manufacturing of exchange linked hard/soft magnetic nano composites. In this study, $SrFe_{12}O_{19}$ (SFO) and $x(CoTm_{0.01}Tb_{0.01}Fe_{1.98}O_4)$ (CoTmTb) (x 3.0) hard/soft ferrites nano composites' structural and microwave properties were also studied (NCS). Magnetization measurements at 300 K (RT) and 10 K in relation to magnetic field measurements were also used to examine the magnetic characteristics (LT). As the soft material at RT rises, magnetic variables such (Mr, Ms, and Hc) exhibit improvement in values. Similar to this, for SFO/3(CoTmTb) NCs, BH max the maximum energy product increases and achieves its maximum value. In the frequency range of 33 to 50 GHz, the SFO/x(CoTmTb) NCs' microwave characteristics were assessed[102].

Table 2-1 Summery of literatures in Hard-Soft ferrite graded

Study Name	**authors**	**Year**
Preparation and studies of Co (II) and Co (III)-substituted barium ferrite prepared by sol–gel method	Teh, G. B., Nagalingam, S., & Jefferson, D. A	2007
Influence of acid catalysts on the structural and magnetic properties of nanocrystalline barium ferrite prepared by sol–gel method	Paimozd, E., Ghasemi, A., Jafari, A., & Sheikh, H	2008
Synthesis and magnetic properties of hard-soft SrFe10Al2O19/NiZnFe2O4 ferrite nanocomposites	Rai, B. K., Wang, L., Mishra, S. R., Nguyen, V. V., & Liu, J. P	2014
Synthesis and magnetic study of magnetically hard-soft SrFe12-yAlyO19-x Wt.% Ni0. 5Zn0. 5Fe2O4 nanocomposites	Neupane, D., Ghimire, M., Adhikari, H., Lisfi, A., & Mishra, S. R	2017
Influence of preparation method on structural, optical and magnetic properties of nickel ferrite nanoparticles	Khan, A. A., Javed, M., Khan, A. R., Iqbal, Y., Majeed, A., Hussain, S. Z., & Durrani, A. S	2017
Synthesis of novel hard/soft ferrite composites particles with improved magnetic properties and exchange coupling	Tavakolinia, F., Yousefi, M., Afghahi, S. S. S., Baghshahi, S., & Samadi, S	2018

Preparation and Identification of BaFe2O4 Nanoparticles by the Sol–Gel Route and Investigation of Its Microwave Absorption Characteristics at Ku-Band Frequency Using Silicone Rubber Medium	Peymanfar, R., Rahmanisaghieh, M., Ghaffari, A., & Yassi, Y.	2018
Investigation of the Structure and Magnetic Properties of Co+ 2–Ti+ 4 Substituted Barium Ferrite Powder Prepared by Sol–Gel Method. In Journal of Physics	Hussain, S. A	2019
Synthesis and magnetic properties of hard/soft SrAl2Fe10O19/Fe (FeCo2) nanocomposites	Kahnes, M., & Töpfer, J	2019
Enhancement on the exchange coupling behavior of SrCo0. 02Zr0. 02Fe11. 96O19/MFe2O4 (M= Co, Ni, Cu, Mn and Zn) as hard/soft magnetic nanocomposites	Algarou, N. A., Slimani, Y., Almessiere, M. A., Baykal, A., Guner, S., Manikandan, A., & Ercan, I.	2020
Phase-and Composition-Tunable Hard/Soft Magnetic Nanofibers for High-Performance Permanent Magnet. ACS Applied Nano Materials	Lee, J., Lee, G., Hwang, T. Y., Lim, H. R., Cho, H. B., Kim, J., & Choa, Y. H.	2020
Enhancement of the maximum energy product in Ba0. 5Sr0. 5Fe12O19/Y3Fe5O12 nanocomposites synthesized by the co-precipitation method	Irfan, H., & Vizhi, R. E.	2020

Alterations in the magnetic and electrodynamic properties of hard-soft Sr0. 5Ba0. 5Eu0. 01Fe12O19/NixCuyZnwFe2O4 nanocomposites	Almessiere, M. A., Slimani, Y., Attia, H., Sheikh, S. I. M., Sadaqat, A., Vakhitov, M. G., ... & Trukhanov, A. V	2021
Review on functional bi-component nanocomposites based on hard/soft ferrites: structural, magnetic, electrical and microwave absorption properties	Almessiere, M. A., Slimani, Y., Trukhanov, A. V., Sadaqat, A., Korkmaz, A. D., Algarou, N. A., ... & Toprak, M. S	2021
Fabrication of exchange coupled hard/soft magnetic nanocomposites: Correlation between composition, magnetic, optical and microwave properties	Slimani, Y., Algarou, N. A., Almessiere, M. A., Sadaqat, A., Vakhitov, M. G., Klygach, D. S., ... & Ercan, I	2021

Chapter Three

3 Experimental procedures

In this chapter, the preparation steps and the raw materials that used to prepare the nano powder ferrite of both types of hard and soft are discussed. This work is conducted in two parts. The first part includes the preparation of nickel ferrite (soft) and barium ferrite (hard), as a pure powders and composite. On the other hand, the second part includes preparation of bulk samples throughout cold pressing in different form, as pure, composite and in the form of layers, figure (3-1) show the steps and parts of work. Finally, series of measurements and tests were done to determine the charactestics of resulted samples.

3.1 Materials and Chemicals.

The materials and chemicals which were used for synthesis nickel ferrite(soft) and barium ferrite(hard) , their purity, and Physical state which are presented in Table (3.1):

Table 3-1 Substances, Chemical Formula, Purity, Source, and the phase state of the Chemicals for start material.

Material name	Chemical formula	Purity	Physical state	Source of the materials
Hydrated nickel nitrate	$Ni(NO_3)_2.6H_2O$	99.5	Solid	Fluka in turkey
hydrate nitrate of iron	$Fe(NO_3)_3.9H_2O$	99.1	Solid	SDFCL in india
Barium nitrate	$Ba(NO_3)_2$	99.1	Solid	Fluka in turkey
Ethylene glycol	$C_2H_4(OH)_2$.	99.0	Liquid	Thomas baker india

Part One

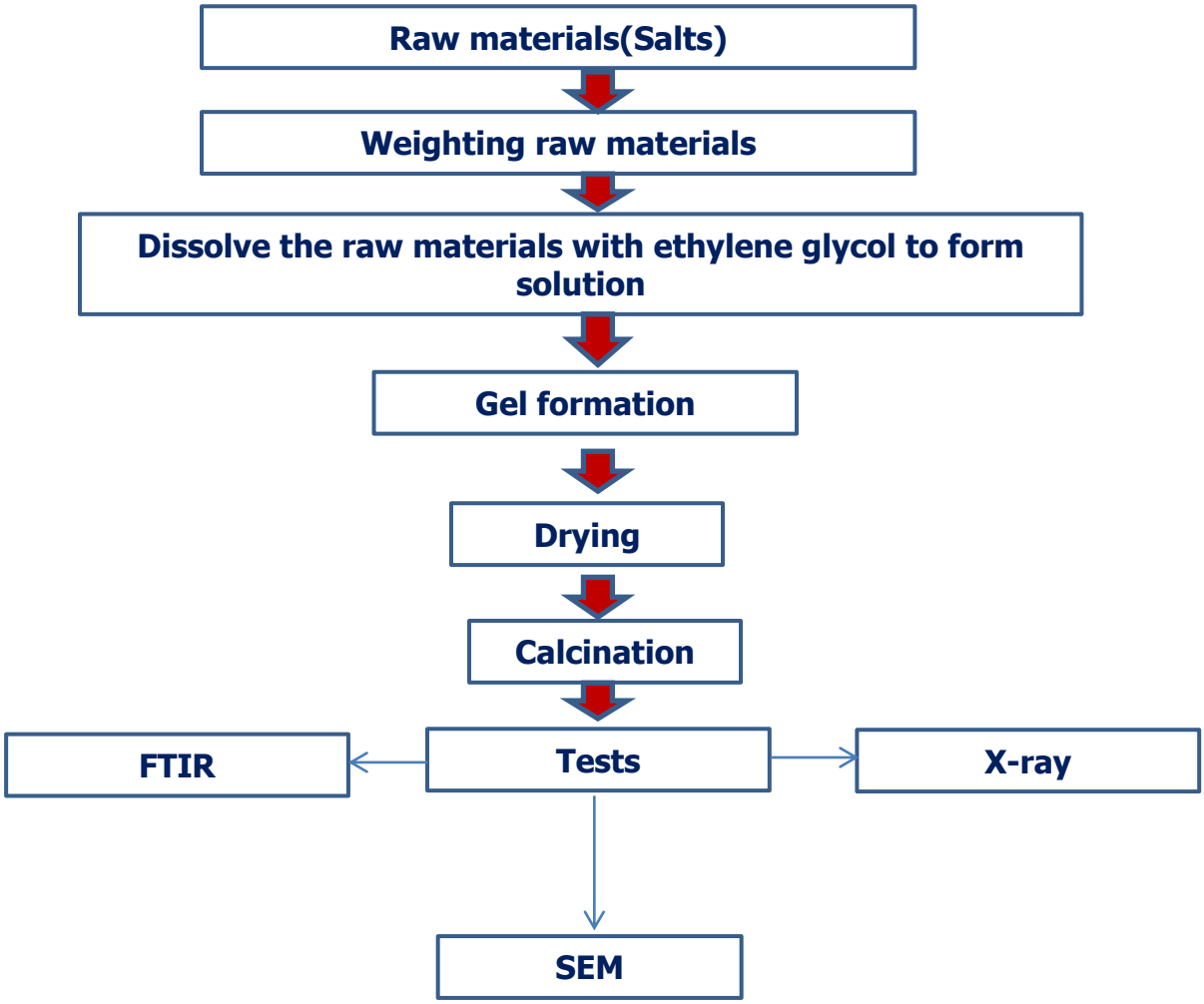
Raw materials(Salts)
Weighting raw materials
Dissolve the raw materials with ethylene glycol to form solution
Gel formation
Drying
Calcination
Tests
FTIR
X-ray
SEM

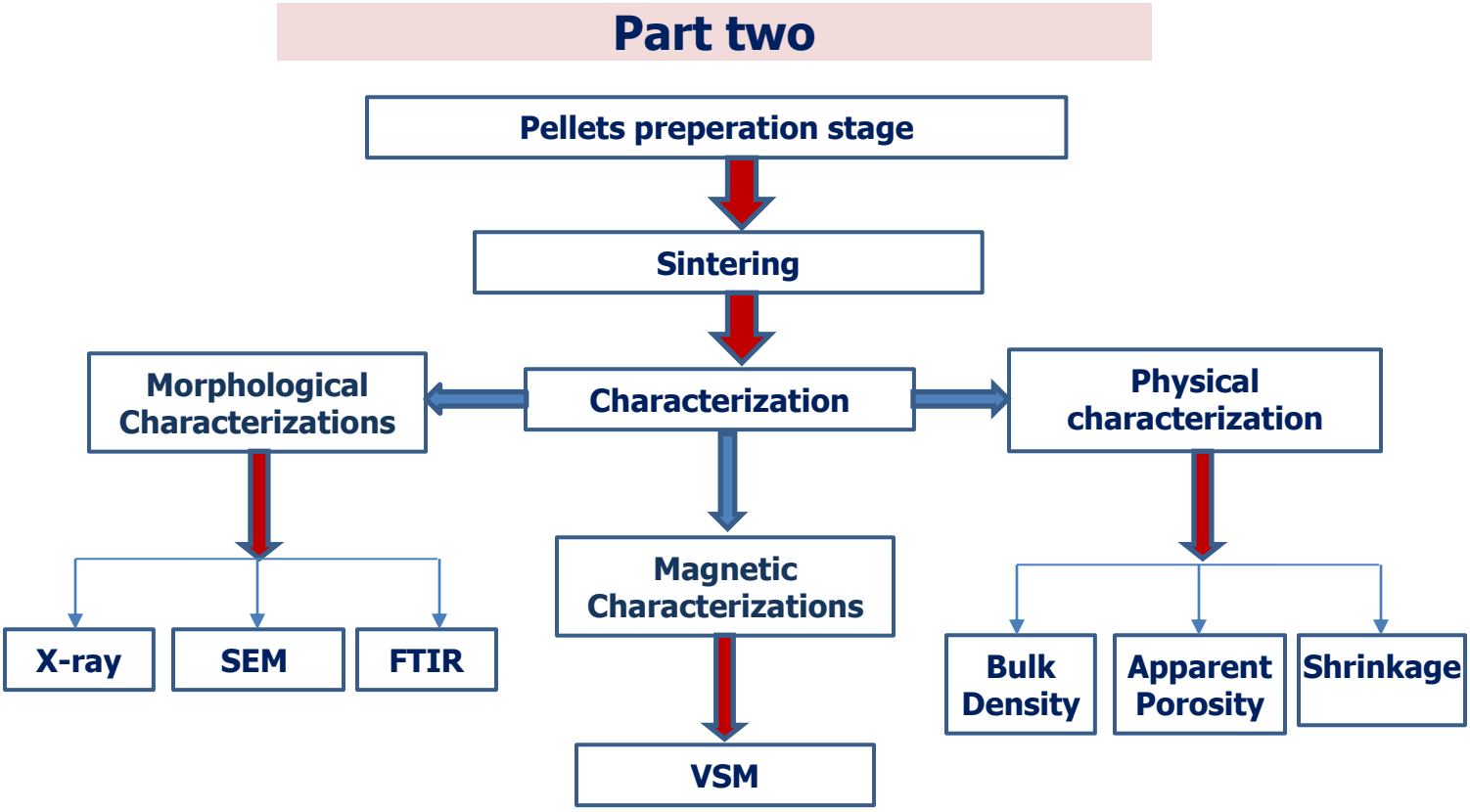

Figure 3-1 Flowchart illustrates the steps and stage of work

3.2 Preparation Ferrite Powders

3.2.1 Preparation Nickel Ferrite (Soft)

In this work, the sol-gel method was used to produce nanopowders ferrite. For nickel ferrite, 2:1 weight ratio of hydrated iron nitrate to hydrated nickel nitrate was dissolved by 100 ml of ethylene glycol. The dissolving process of (hydrated iron nitrate) and (hydrated nickel nitrate) was achieved separately in 50 ml of ethylene glycol for each one, using magnetic stirrer for 1 hour to ensure a complete dissolution of iron nitrate granules, figure(3.2) isolated the steps to produce powder of nickel ferrite. Both solutions are mixed by the stirrer for one hour. Then the temperature of the stirrer is raised to 120°C for 5 hrs in order to obtain a brown gel. Prior drying, afterwards, the gel dried at a temperature 190 °C for 7 hours. Then, it was calcined at 600 °C for 5 hrs at a rate of 5 °C/min, using furnace (JYMF-1800, High Temperature Muffle Furnace) at the Department of Ceramic engineering and Building Material / College of Engineering Materials/ University of Babylon.

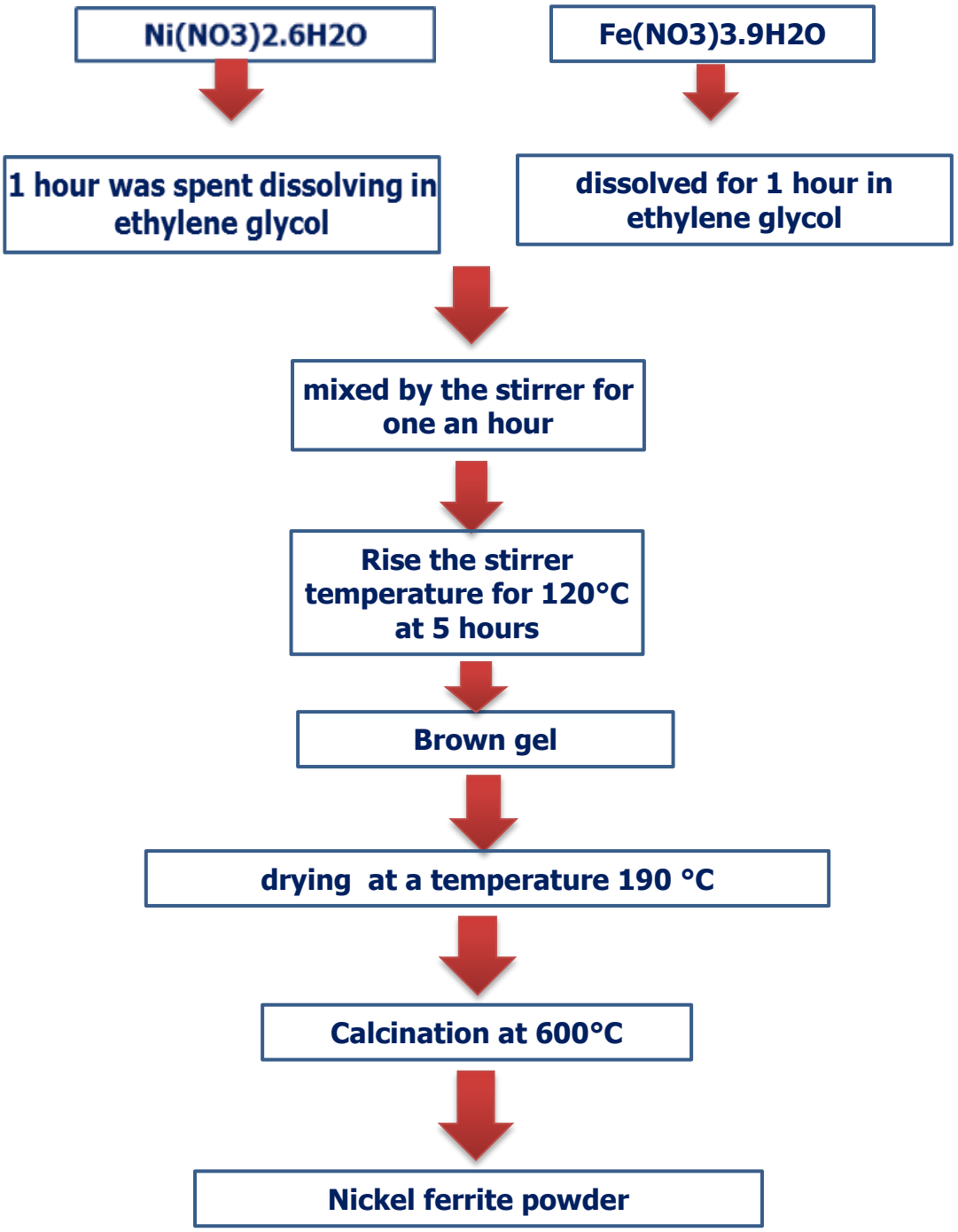

Figure 3-2 Flowchart Illustrate the Steps to Prepare nickel ferrite powder.

3.2.2 Preparation barium Ferrite(hard)

As in nickel ferrite , barium ferrite prepared by a sol-gel method in order to obtain the powder, where 2:1 weight ratio of iron nitrate hydrated to barium nitrate were 100 ml of ethylene glycol used to dissolved, steps of produce powder of barium ferrite as illustrated in figure(3.3). The dissolving process of (hydrated iron nitrate) and (barium nitrate) was achieved separately in 50 ml of ethylene glycol for each one, using magnetic stirrer for one hour to ensure a complete dissolution of iron and barium nitrate granules using a magnetic stirrer and after that, add the first solution of barium nitrate gradually to the second solution consisting of iron nitrate and mix both solutions together for one hour to obtain a homogeneous solution, temperature of the stirrer is raised to 120°C for 5 hrs in order to obtain a gel. Afterwards, the gel dried at a temperature 190 °C for 7 hours. Then, it was calcined at 800 °C for 5 hrs at a rate of 7 °C/min, using furnace (JYMF-1800, High Temperature Muffle Furnace) at the Department of Ceramic engineering and Building Material / College of Engineering Materials/ University of Babylon.

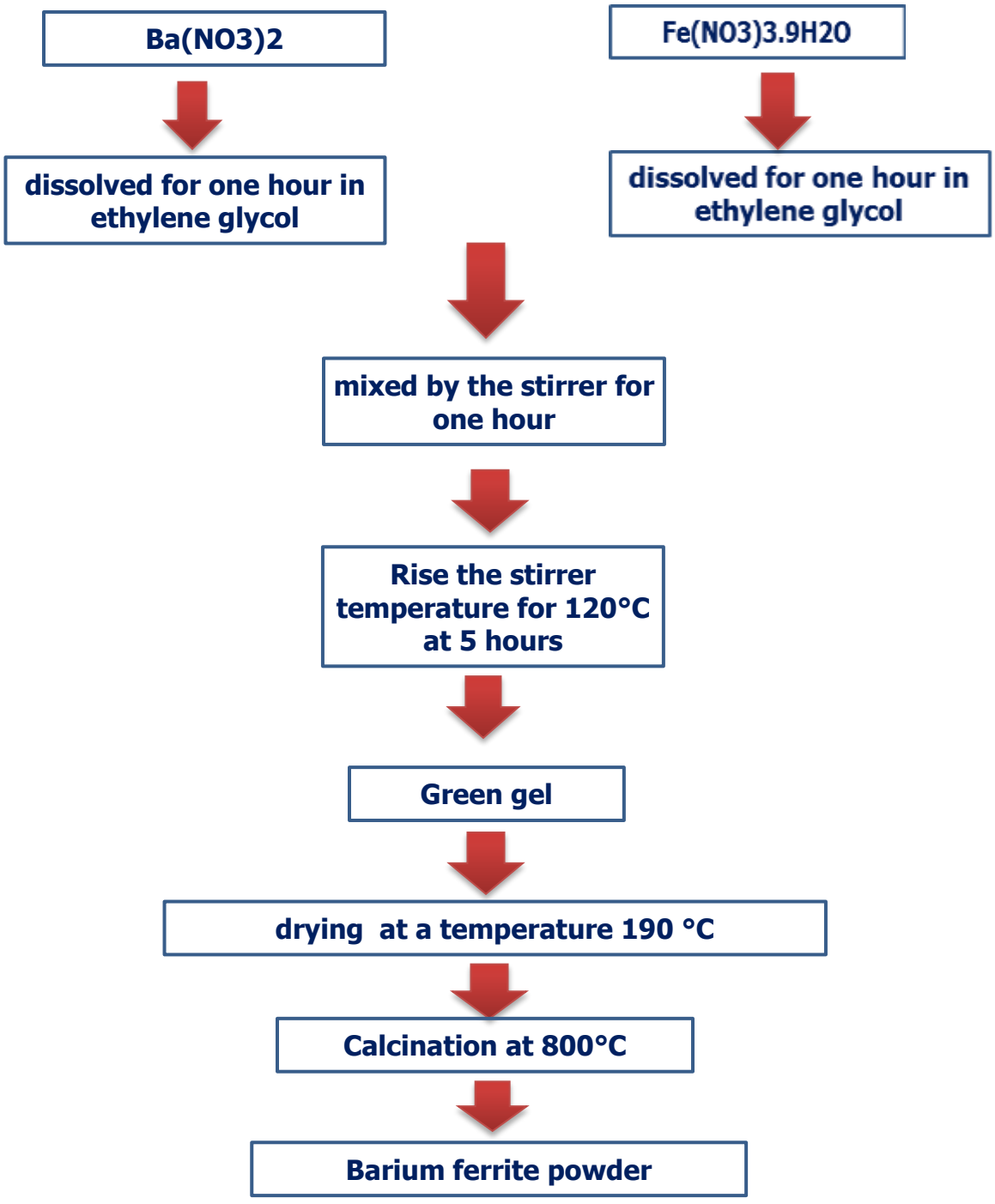

Figure 3-3 Flowchart Illustrate the Steps to Prepare Barium ferrite powder.

3.3 Composite particles hard –soft ferrites

In the present work , hard(barium ferrite)/ soft(nickel ferrite) , sol-gel was used to create the composite particles. After the solutions have been prepared as mentioned previously in the previous two paragraphs, specific proportions are taken from both solutions (25BF/75NF, 50B/50NF, 75BF/25NF) for the preparation of composite ferrite

The nickel ferrite solution heated at 60°C to get a brown solution by a magnetic stirrer was then added to the first beaker containing barium hexaferrite salts after being transformed into a light green solution , then mixed at 120°C for 5 hours by magnetic stirrer, after that start formation a viscous gel. The gel then dried in the oven at190 °C for 7 hours , creating the dark colored powder.

After the process of preparing powders for (nickel ferrite) and (barium ferrite), by the sol- gel method and calcination in an electrical digital furnace(JYMF-1800, High Temperature Muffle Furnace) was used to calcination all powders that prepared at (800° C to composite powder) with heating rate 7° C/ min .

3.4 preparation of bulk samples

3.4.1 Preparation pellets ferrite

To prepare the pellets of ferrites as sintered samples for different measurements, the produced powders are pressed in two ways. First, pure pellets were produced of (nickel ferrite, barium ferrite and composite). Secondly, sample was produced as layers ferrite from pure nickel ferrite (soft) and barium ferrite (hard), as presented in table(3-2).

Pressing process is performed throughout press the dry powder was pressed uniaxially into pellets with a pressure of 150 MPa for 40 s in a cylindrical stainless steel die. The diameter of the pellets was 10 mm, while the thickness varied from 0.9 to 1.2 mm, according to requirements of the corresponding magnetic measurement. Pressing layers of ferrite after sintering shown in figure (3-4).

For sintering, the pellets were placed onto a thin layer of zirconia sand (baddeleyite sand) and covered by an alumina crucible. The sintering process carried out in two stages . Firstly, heating the pressed samples up to 600 ^{o}C for 2 h with heating rates of 5 ^{o}C/min-1. Then, they heated up to 1200 ^{o}C for 2 h with same heating rates.

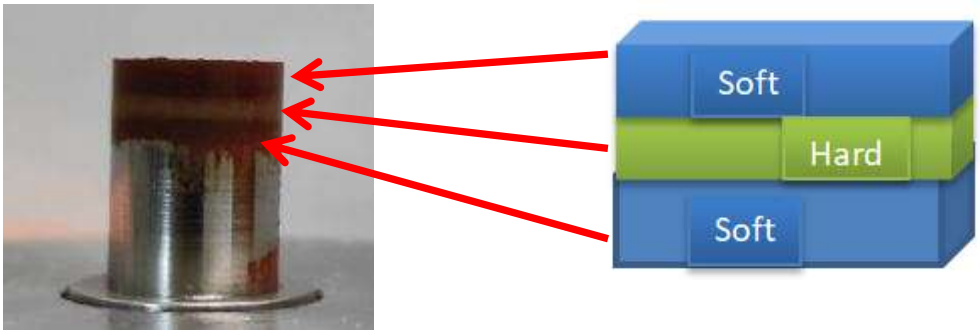

Figure 3-4 Ferrite layers

Table 3-2 materials and forms of prepared samples

Type	Material and form
(Soft)	100 % Nickel Ferrite
(Hard)	100 % Barium Ferrite
Composite ferrites	75 % Nickel Ferrite (Soft)+ 25% Barium Ferrite (Hard)
	50 % Nickel Ferrite (Soft)+ 50% Barium Ferrite (Hard)
	25 % Nickel Ferrite (Soft)+ 75% Barium Ferrite (Hard)
Layers of ferrites	Soft+ Hard+ Soft

3.5 Morphological and Microstructure Characterization

This section provides the essential characterizations of the ferrite nano powder following production to establish the characteristics of the finished products, which includes:

3.5.1 X-ray diffraction Analysis

crystallographic structure and hence identify unidentified materials. In order to detect any crystalline phases, as well as whether the structure is amorphous or crystalline,, samples are finely ground and scanned on a Cu k radiation (= 1.5405)- using x-ray diffract meter (XRD 6000, Shimadzu, Japan) operating at the ceramics labs of the College of Material Engineering at the University of Babylon at a scanning rate of 5 °/min from 20° to 80° of 2Ɵ (Bragg angle), and with When the circumstances are right, the sample's interaction with the incident photons produces diffracted rays and constructive interference. Using the Joint Committee for Powder Diffraction Standards Data (ICCD) as a reference, the phases that were present were determined [103].

3.5.2 Scanning Electron Microscopy (SEM) Analysis

The produced samples (nickel ferrite/barium ferrite samples) are used to provide information on the morphology using the powerful technology known as SEM. The samples in this study were polished, put on display, and then covered in a very thin coating of gold by depositing that use the sputter technique to establish a line of conduction for the aim of preventing ion charging on the specimens. By introducing a voltage difference between the anode and the filament (cathode), the tungsten filament in a SEM is used to generate an electron beam that travels through vacuum. By using electromagnetic lenses to concentrate it, the beam was then directed downward toward the sample surfaces. While interacting with the sample, this beam scanned (moved back and forth over the selected area of the sample), causing the electrons to get dislodged from the atoms. The resolved,

detected, and then exhibited on a screen electrons that result from the interaction[105]

SEM instrument (VEGA 3 SBU) in the ceramics laboratories / College of Material Engineering/ University of Babylon .

3.5.3 FT-IR Analysis

The FTIR was employed to determine the presence of Bariun and Nikel ferrites both before and after sintering . Vibrational frequency between the bonds is represented by the absorption peaks in the FTIR spectrum. FTIR an indication to the type of materials from the intensity of bands , making FTIR a great tool for qualitative investigation [106] The FTIR - 8300 spectrometer, which was employed for the test and is accessible at the polymer labs of the College of Material Engineering in the University of Babylon.

3.6 Vibrating Samples Magnometer (VSM) Measurement:

Materials' magnetic characteristics are measured using vibrating sample magnetometer (VSM) devices as a function of magnetic field [107]. The saturation magnetization (Ms), the remanence (Mr), and the coercivity (Hc) are the three retrieved parameters from the hysteresis loop that are most frequently employed to describe the magnetic characteristics of magnetic medium. A vibrating sample magnetometer works on the fundamental tenet that a changing magnetic flux will cause a voltage to be produced in a pickup coil [108]. VSM test used to identify the magnetic characteristics of ferrites nanoparticles . The test was performed using a model (Cryogenic VSM) in Tehran, Iran.

3.7 Physical Characterization of ferrite

According to (ASTM C373-88) [109], apparent porosity and bulk density were measured using the Archimedes technique as follows:

1. Measuring the dry mass (D) after the sample has been dried at 150°C for 24 hours and has cooled to room temperature (D).

2. After boiling for 5 hours, the test sample was placed in a beaker and filled with distilled water. It was then allowed to soak for an additional 24 hours before the suspended mass (S) was measured.

3. Immediately following the determination of (S), The excessive water was cleaned off the sample using a damp cotton towel before the saturated mass (M) was measurement. The following calculates of apparent porosity:

Apparent Porosity (%)=$\frac{M-D}{M-S}$*100……. (3.4).

Bulk density calculated using the equation below

Bulk density=$\frac{D}{M-S}$ ……(3.5)

The following equation measures the shrinkage that occurs to the samples after sintering :

shrinkage% = $\frac{D1-D2}{D1}$∗100 ……...(3.6)

where D1 is the diameter of the test item before shrinking. D2 is the specimen's dimension following shrinking.

Chapter Four

4 Results and Discussion

In this chapter the data gained from the aforementioned measurements for all produced samples will be demonstrated and discussed in details. In addition they will be compared to access the obtained properties.

4.1 Structural Characterization

4.1.1 X-Ray Diffraction Analysis.

Prior to and following sintering, the generated Nickel ferrite powder is examined. Figure (4. 1) illustrates X-ray diffraction pattern for 100%$NiFe_2O_4$ before sintering spinel nanoparticles that were calcined at 600 °C measured at 2θ in range of (20° - 80°). It is evident that there is no second phases were formed and the main characteristics peaks are appeared which are 30.578, 35.978, 37.378, 43.678, 53.988, 57.628, and 63.098, respectively, correspond to the (2 2 0), (3 1 1), (2 2 2), (4 0 0), (4 2 2), (5 1 1). It classified as inverse spinel with crystal structure of face-centered cubic (FCC) and can be indexed under ICCD (Card No. 10-0325). This result is consistant with previous study [110].

Afterwards, X-ray diffraction for sintered samples 1200 °C was taken for 100% $NiFe_2O_4$, as presented in figure (4. 1). it exhibited that the primary peaks are more sharp with high intensity which indicates to high crystallinity.

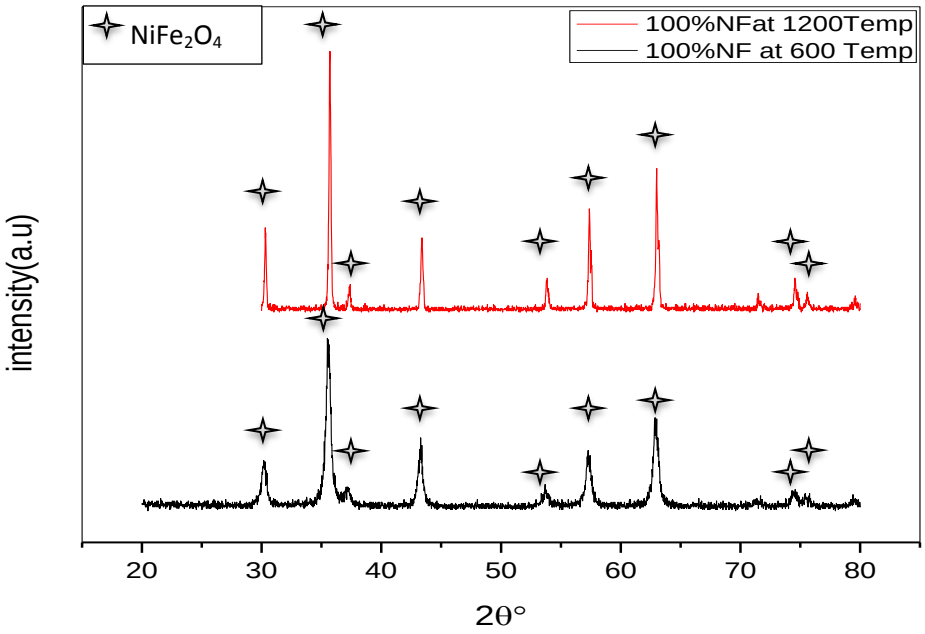

Figure 4-1 XRD analysis for Nickel samples at 800°C and 1200°C

The XRD Pattern of nanocomposite powder for proportions 75NF/25BFof nickel ferrite / barium ferrite before and after sintering process are shown in Figure(4.2) The XRD Pattern clearly illustrates the production of composite phases. It can be seen that when the $NiFe_2O_4$ concentration in the NF-BF composite increases at 800^{o}C the intensity of peak corresponding to the nickel ferrite phase gets increases will be increased matched with card number [10-0325].

At temperature 1200 °C, XRD and a crystalline phase of it shown in figure (4.3), where each of the peaks of the two materials appeared .The result of the composite nanopowder when the ratio of nickel ferrite to barium ferrite 75/25 it is matched with card number [10-0325] for nickel ferrite , and [00-025-1191] for barium ferrite

In figure (4.2) The x-ray analysis shows the composite materials with a ratio of nickel ferrite to barium ferrite is 25NF/75BF . The analysis shows the presence of both barium and nickel ferrites peaks, but they are peaks of barium ferrite with the phases ($BaFe_2O_4$) more than peaks of nickel ferrite , is matched with card number [00-044-0897] for barium.

The result of the composite nanopowder at temperature 1200 °C when the ratio of nickel ferrite to barium ferrite 25NF/75BF is matched with card number [00-025-1191], shown in figure (4.3). Where shown the other phases of barium ferrite , appear the two phases of barium there are ($BaFe_2O_4$ and $BaFe_{12}O_{19}$) with a little peaks of nickel ferrites This result is contestant with previous study [111] [112].

In figure (4.2) when the ratio of nickel to barium 50NF/50BF , There are barium ferrite peaks with hexagonal phases and $NiFe_2O_4$ spinal structures. The XRD peaks seem to vary in intensity as The XRD data show a concentration of either $BaFe_2O_4$ or $NiFe_2O_4$, but no additional unidentified peak. Using pure data, all of the peaks are indexed. $BaFe_2O_4$ and pure $NiFe_2O_4$ to show the presence of both barium ferrite and nickel ferrite at 800°C.

XRD at temperature 1200 °C revealed nickel and barium ferrite with a ratios 50NF/50BF . The result of composite powder matched with card number [01-074-2081] for barium and [00-044-1485] for nickel ferrite shown in figure (4.3) .which show the main peaks of barium and nickel ferrites with high crystallite and sharp , where shown two phases of barium ($BaFe_2O_4$, $BaFe_{12}O_{19}$) . The relative weight ratio of the soft and hard phases affects the diffraction peak intensities of the (barium and nickel)phases. No additional phases were seen within the x-ray diffraction patterns' resolution limit, showing that the two parent phases (soft and hard ferrite) could exist in the two-phase nano composites and that

they had high chemical compatibility . This result is contestant with previous study [111] [112].

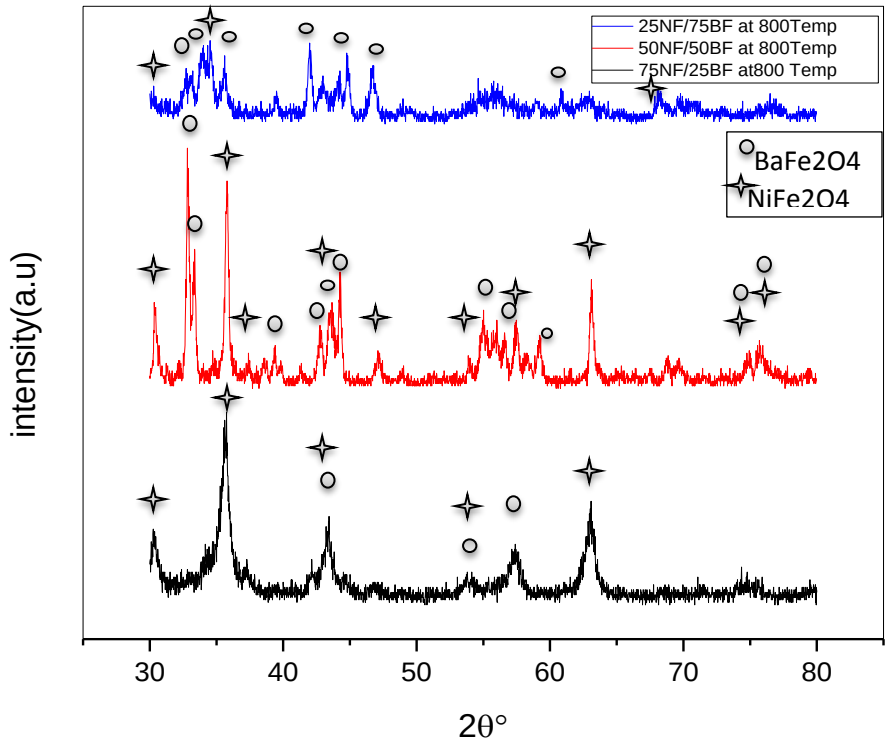

Figure4.2 XRD analysis for composite ferrite samples at 800°C

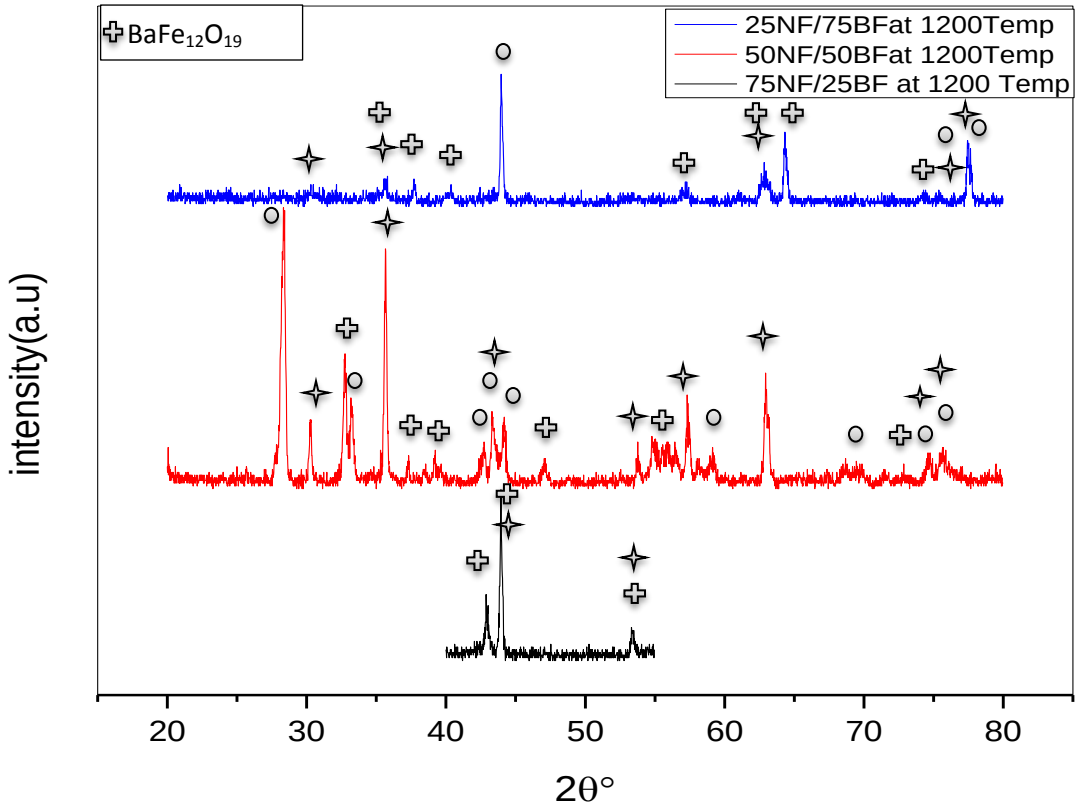

Figure4.3 XRD analysis for different samples at 1200°C

The XRD pattern of the100%BF (barium ferrite) powder produced at 800℃ is shown in Figure (4-1). Various miller indices, including (212), (610), (020), (422), (213), (614), and (232).calcination temperature from at 800°C, crystalline phases disappeared and a barium ferrite with phase of $BaFe_2O_4$ nanoparticles was synthesized. This deals with the source [113].

The diffraction patterns (XRD) for 100%barium ferrite after sintering are shown in figure (4-4) The identification (creation) of barium ferrite peaks is seen more shaped and clearly at 1200 °C, according to the XRD data. Another phases of barium ferrite is ($BaFe_{12}O_{19}$) may also be seen in the sample with barium ferrite phase ($BaFe_2O_4$) This agree with Ref [112].

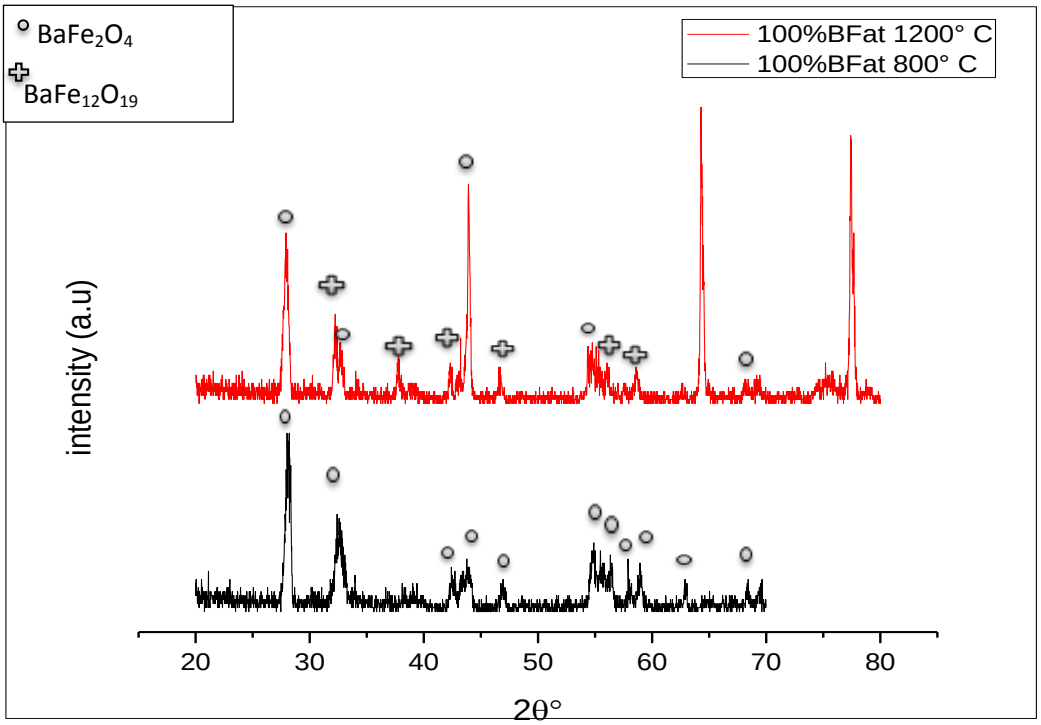

Figure4.4 XRD analysis for Barium ferrite samples at 800°C and 1200°C

4.1.2 Scanning Electron Microscope (SEM) analysis .

SEM images of nickel ferrite $NiFe_2O_4$ the shown in figure (4.5. a, b) at 600°C and at 1200°C .

The samples of nickel ferrite nanoparticles are coated by gold in order to avoid the charging effect. SEM images indicate there are micrometrical agglomerate of very fine of $NiFe_2O_4$ particles as those nanoparticles have high surface energies, SEM images in figure (4.5.a) are shown the spherical shape of the nickel ferrite powder found the particular size of powder at 600°C ranges ~300nm where shown in table (4.1).

For pressed sample after sintering at 1200°C The SEM micrographs show that the obtained $NiFe_2O_4$ the grain size increase due to the growth of particles with increasing temperature . As can be seen clearly in figure (4.5 b) the images are shown some porosity. This is found with the previous study [114].

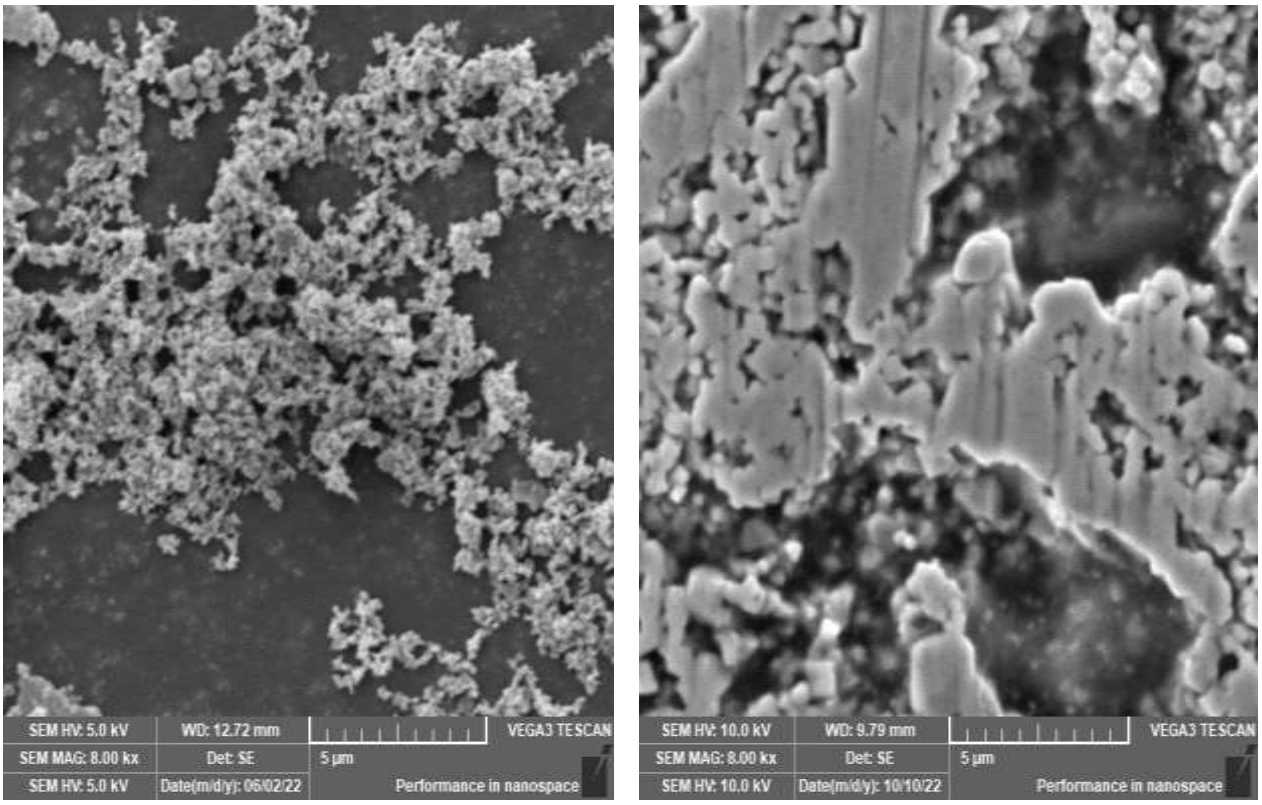

(a) (b)

Figure 4-5 SEM images: a- NiFe2O4 at 600 °C, b- NiFe2O4 at 1200 °C

SEM of compost hard/soft ferrite with different proportions the shown in figure (4.6 a, b, c , d) . the SEM images of the composite material with a ratio of 50/50 of nickel ferrite and barium ferrite shown in figure (4.6 a) showed The powder at 800 °C , The identification shape of composite powder show quasi spherical particles ,indicates a normal distribution of both magnetic phases in the sample.

Typical SEM images after sinteringg at 1200 °C as show in figure (4.6, b). All images show two distinct phases, Most barium ferrite grains have shape of a granule, after the sintering process is the growth of the granules, as well as for the granules of nickel ferrite, and note that there is very little pores in the sample after the sintering and pressing process

In the figure (4.6, c) shows the SEM images of the sample in which the ratio of nickel ferrite to barium ferrite is 75/25, where the images appear after sintering and pressing processes.

The same is the case with the shape(4.6 ,d) where the percentage of nickel ferrite to barium ferrite is 25/75, and notice the presence of Pores spread between the two phases after the sintering process, This result is contestant with previous study [111] . Where the particles size of all samples shown in a Table (4.1).

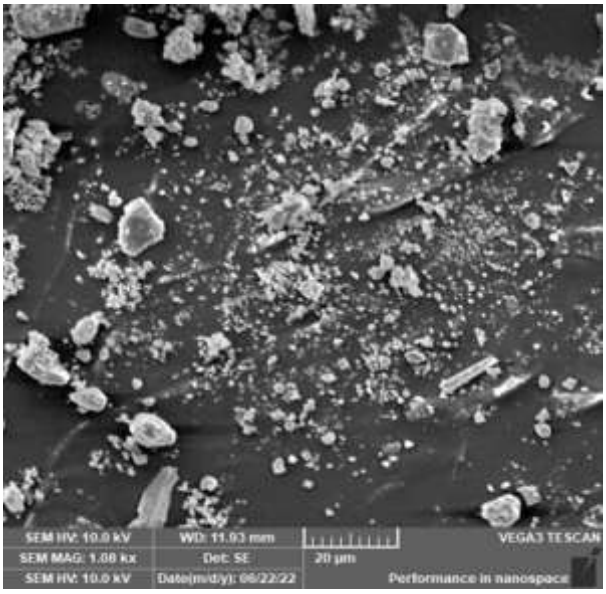

(a)

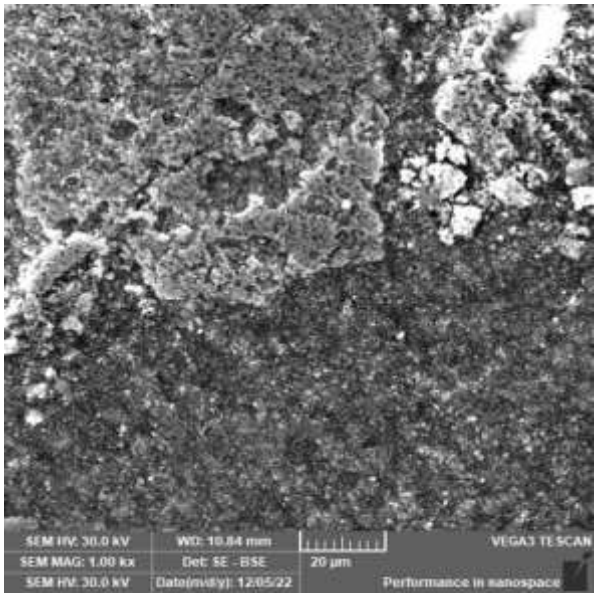

(b)

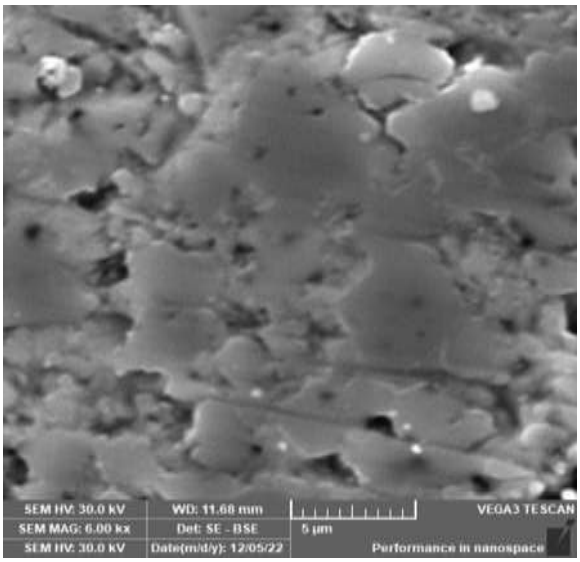

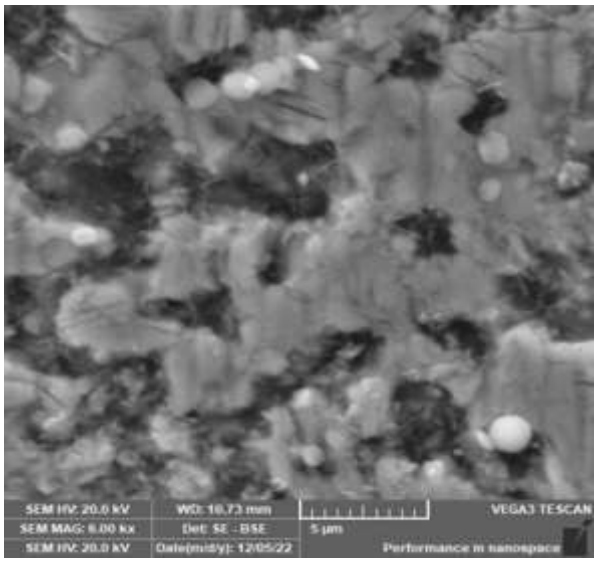

(c) (d)

Figure 4-6 images SEM : a- nano composite with ratio 50/50 at 800 °C, b- nano composite with ratio 50/50 at 1200 °C C – nano composite with ratio 75/25 nickel ferrite / barium ferrite at 1200 °C d - nano composite with ratio 25/75 nickel ferrite / barium ferrite at 1200 °C

SEM images of barium ferrite the shown in figure (4.7. a, b) at 800°C and 1200°C after sintering . Figure (4.7,a) shown barium ferrite at 800°C SEM pictures show a needle-like shape. found the particular size of powder at 800°C ranges ~800nm where shown in table. (4.2) The interactions of the barium ferrite's magnetic particles lead to agglomeration so can also be seen that a little of agglomeration has occurred . For pressed sample after sintering at 1200°C The SEM micrographs show in figure (4.7,b) , the shape and grain size of the pure barium ferrite samples that were produced. With rising temperature, the grain size increasing .The air gap between the barium ferrite particles is rather considerable;

this characteristic is mostly utilized to identify the material's porosity . that accepted with Ref [115].

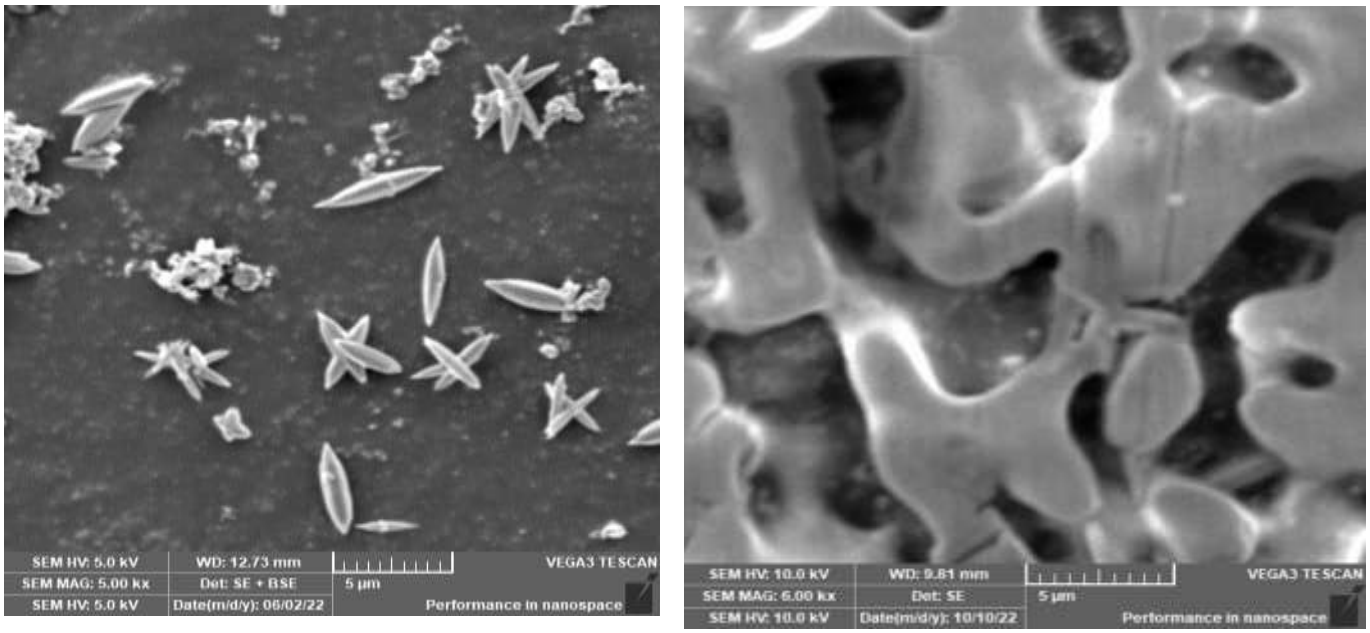

(a) (b)

Figure 4-7 SEM images: a- $BaFe_2O_4$ at 800 °C, b- $BaFe_2O_4$ at 1200 °C

SEM of layers ferrite , hard (barium ferrite) and soft ferrite (nickel ferrite)are shown in figure (4.8 a , b) . The images show two types of layers, where the middle layer represents barium ferrite (hard ferrite) and the side layers represent nickel ferrite, where notice from the images absence of separation of the layers, where the SEM images show the presence of pores in each of the two layers, as well as the occurrence of granular growth after the sintering process.

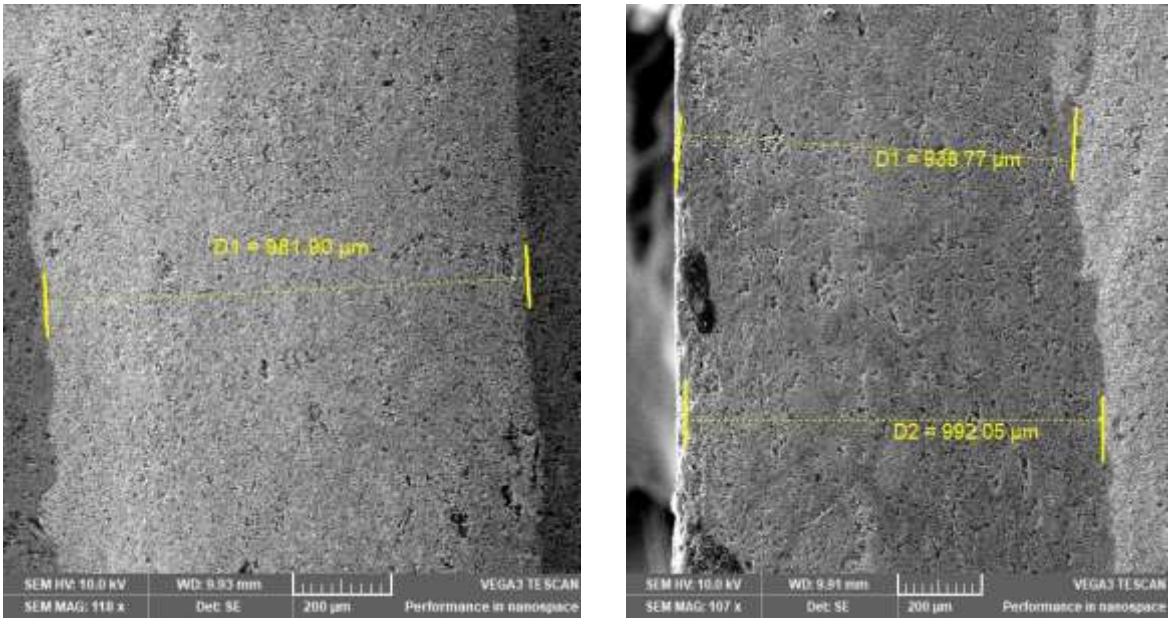

(a) (b)

Figure 4-8 SEM images: a- Barium ferrite layer at 1200 °C, b- Nickel ferrite layer at 1200 °C

Table 4-1 particles size of samples at 600°C and 1200°C

Samples Nickel ferrite /Barium ferrite	Particles size at 600,800 °C from particle size analyzers	grain size at 1200 °C from the SEM image
100%Nickel ferrite	~300nm	589-353 nm
100%Barium ferrite	~800nm	3740-9593 nm
Composite ferrite with ratio 50/50	——	8006-11345 nm
Composite ferrite with a ratio 75/25 ,NF/BF	——	822-1451 nm
Composite ferrite with a ratio 25/75,NF/BF	——	787-3747 nm

4.1.3 FT-IR analysis.

The FT-IR spectrum of nickel ferrite nanoparticles is shown in Figure (4-9), with curves (a) and (b) denoting pre- and sintering, respectively. The NiFe2O4 nanoparticles typical FTIR spectra are shown two peaks that are below 1000 cm-1 and are measured between 400 and 4000 cm-1. The vibration of ions in the crystal lattice is typically attributed to the FT-IR bands of solids. The Figure (4-9 a) all spinels, particularly ferrites, exhibit two primary wide metal-oxygen bands in the infrared spectrum with wavenumbers between 1000 and 400 cm-1. The higher one (v1), which is often detected in the range of 630-550 cm-1, is brought on by the tetrahedral metal-oxygen bond's stretching vibrations. The vibrations of metal and oxygen at the octahedral sites produce the lowest band (v2), which is often found in the range 450-390 cm-1. The H-O-H bending vibrations and stretching modes of the free or absorbed water are ascribed to the spectra's conspicuous bands between 3400 and 1600 cm-1. Figure (4-9, b) depicts the annealed $NiFe_2O_4$'s FTIR spectrum. The 420 cm-1 and 600 cm-1 absorption bands are the only two available. Such a conclusion we find close to the source [116].

which, in the spinel compounds, are octahedral and tetrahedral metal-oxygen stretching vibrations, respectively [117]

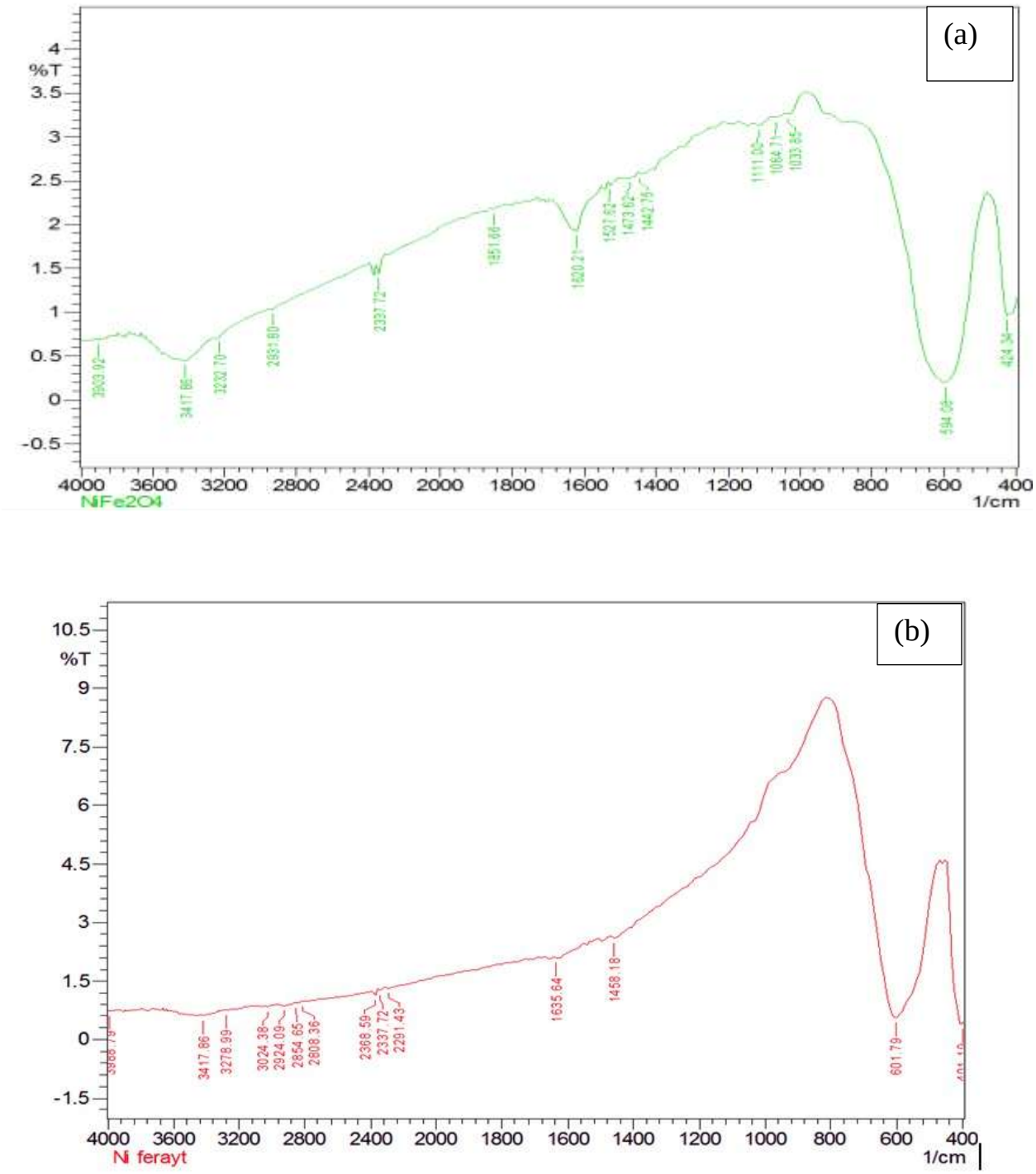

Figure 4-1 a- FTIR OF $NiFe_2O_4$ at 600 °C, b-FTIR OF $NiFe_2O_4$ at 1200 °C

The FT-IR spectra of barium ferrite is seen in Figure (4-10). after sintering at 1200 °C 620 cm-.1 and 862 cm-.1 characteristics peaks connected to a stretching vibrations of Fe^{+3}-O-2bond and Ba^{+2} O-2bond, respectively. The stretching and bending vibrations of the O-H bond were thought to be responsible for the peaks at 1440 cm-1, 1639 cm-.1, and a wide band at 3354 cm-1. The presence of absorbed water molecules on the surface of barium ferrite nanoparticles was associated with the OH peaks.

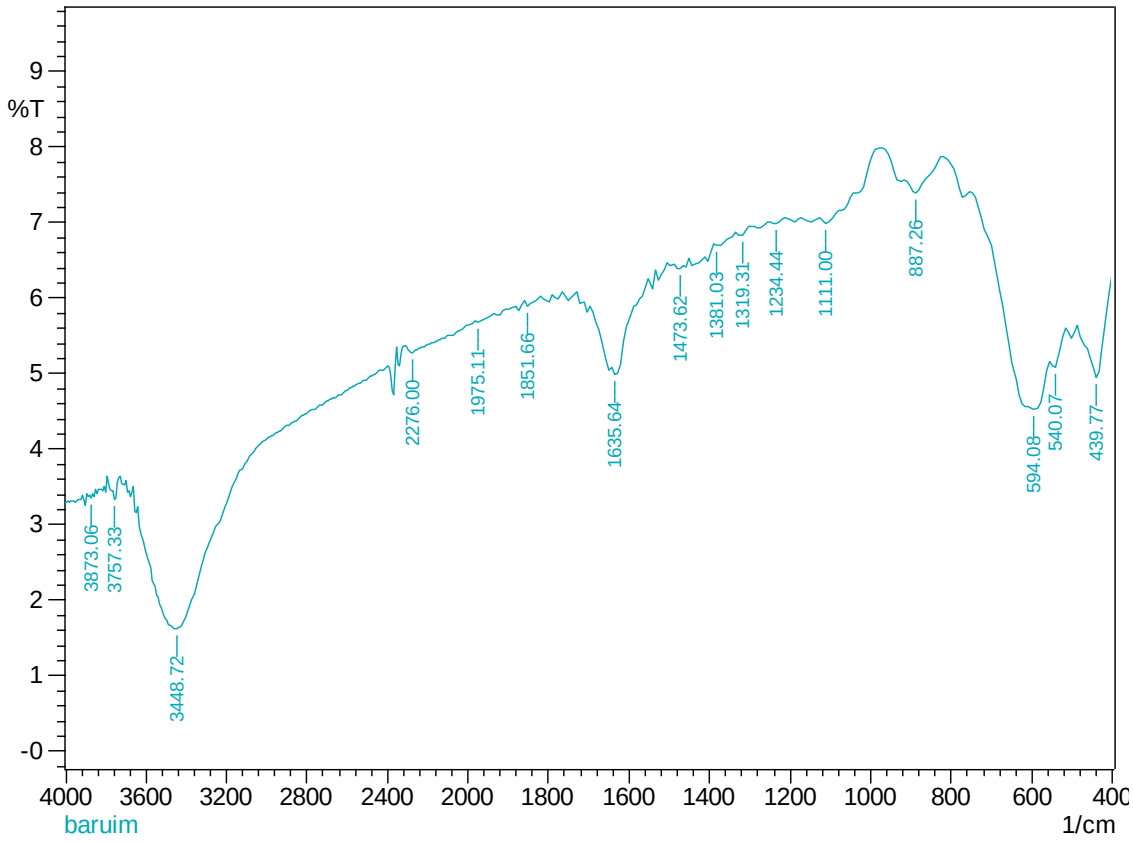

Figure 4-2 FTIR of Barium ferrite at 1200 °C

The FT-IR spectrum is shown in Figure (4-11) of composite nickel/barium ferrites at 1200 °C ,in the range of 400 cm-1 to 4000 cm-1 for composites , This figure supports the structural details of the creation of composites that was previously described using XRD patterns. The composites' spectra exhibit absorption bands at wavelengths of 440 cm-1, 541 cm-1, and 595 cm-1. The stretching vibration of the M-O bonds form at the tetrahedral location is cause of high-frequency band between 570 and 610 cm-1. Additionally, the bands between 390 and 440 cm-1 have a connection to the vibration of metal and oxygen at the octahedral site. The presence of bands in samples supports the ferrites structure's creation in produced nanocomposites. These bands clearly alter somewhat when the hard/soft content ratio rises, which may be a result of hard and soft phases coupling in composites.

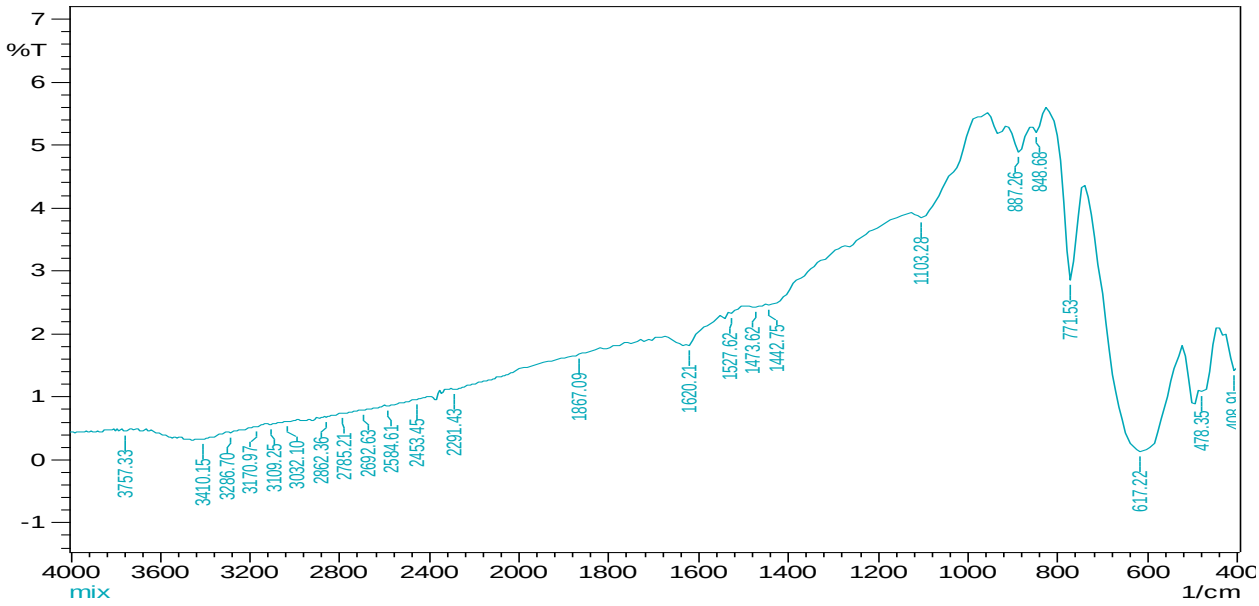

Figure 4-3 FT -IR spectrum composite nickel/barium with ratio 50/50 ferrites at 1200 °C

4.2 Vibrating Samples Magnometer (VSM) measurement:

VSM is used to perform magnetic characterization of the samples at room temperature with the highest possible applied field of 10,000 Oe. Figs. (4.12) (4.13 a, b, c),(4.14), (4.15) show typical magnetic hysteresis loops for a soft ferrite , composite ferrite, hard ferrite , layers sample all of them sintering at 1200ºC for. Table (4.2) shows the magnetic properties of nanoparticals .

Figure(4.12) The hysteresis loop obtained is a "S" shape curve that shows the material's soft superferromagnetic behavior. A look at the hysteresis curve reveals it. The magnetic saturation (Ms) is high for soft ferrite and coercivity (Hc) of sample is lower . Because of the steady rise in crystallinity and particle size, raising the calcination temperature has an impact on the saturation of magnetic values, This agrees with Ref [118]. As the temperature rises, the saturation magnetization (Ms) increases[119]. Were finding the Ms for nickel ferrite is (39.586 emu/g) it is higher than the other samples , lower coercivity Hc is (28.499)

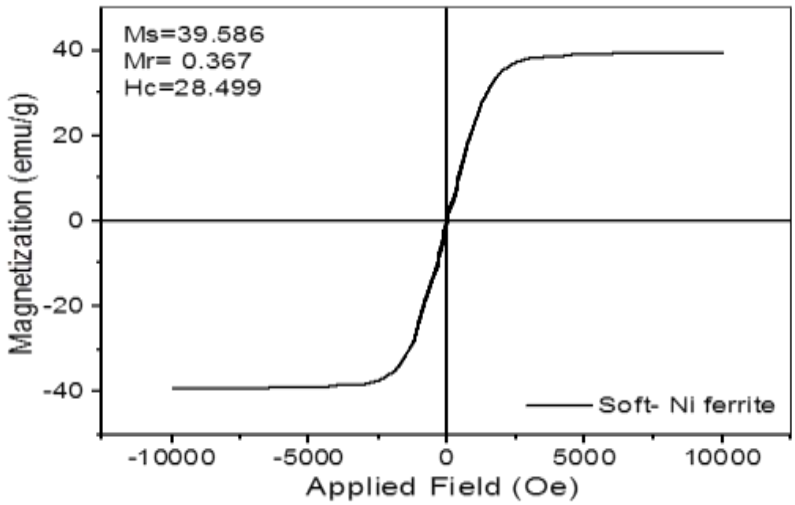

Figure 4-4 hysteresis loop of soft ferrite .

To investigate the behavior of the produced ocomposites', room-temperature hysteresis loops were obtained, Figure (4.13 a) shows hysteresis loop of the soft /hard with ratio 75NF/25BF ferrite sample sintering at 1200°C. This sample's single smooth hysteresis loop. However, Along with the dipolar interaction, the exchange interaction also plays a significant role in the coercivity of the soft phase, since it dropped as the weight ratio of the soft phase increased. Barium ferrite has a substantially coercivity than Nickel spinel ferrite .As a result of adjacent moment in hard/soft systems, additional a demagnetizing field lowers the nanocomposites' total Hc. In other words, the importance of the dipolar interactions among the soft grains grows with the quantity of spinel phase. Here, coercivity is reduced by nucleation of the reverse domains in the soft phase with low nucleation field.

The Mr/Ms ratio of the nickel ferrite /barium ferrite a sample of a nanocomposite was discovered to be high It dropped as the soft magnetic content rose. The interaction at hard/soft grain interface gradually decreased as amount of soft-magnetic phase rose as a result of the exchange coupling decreasing, This agrees with Ref [111].

To rise both the alignment and the magnetization of magnetic systems, both hard and soft, exchange interaction really aids in aligning , magnetic moments of hard and soft phases are parallel, can be shown in figure (4.13, b).

Figure (4.13 c) demonstrates the hysteresis loops of the soft/hard ocomposite powders ,ratio 25NF/75BF ferrite at 1200°C. This sample's single hysteresis loop, which indicates between the hard and soft phases, there is a significant exchange coupling, can be observed clearly. The corictivity increased as the amount of hard magnetics phase increased .

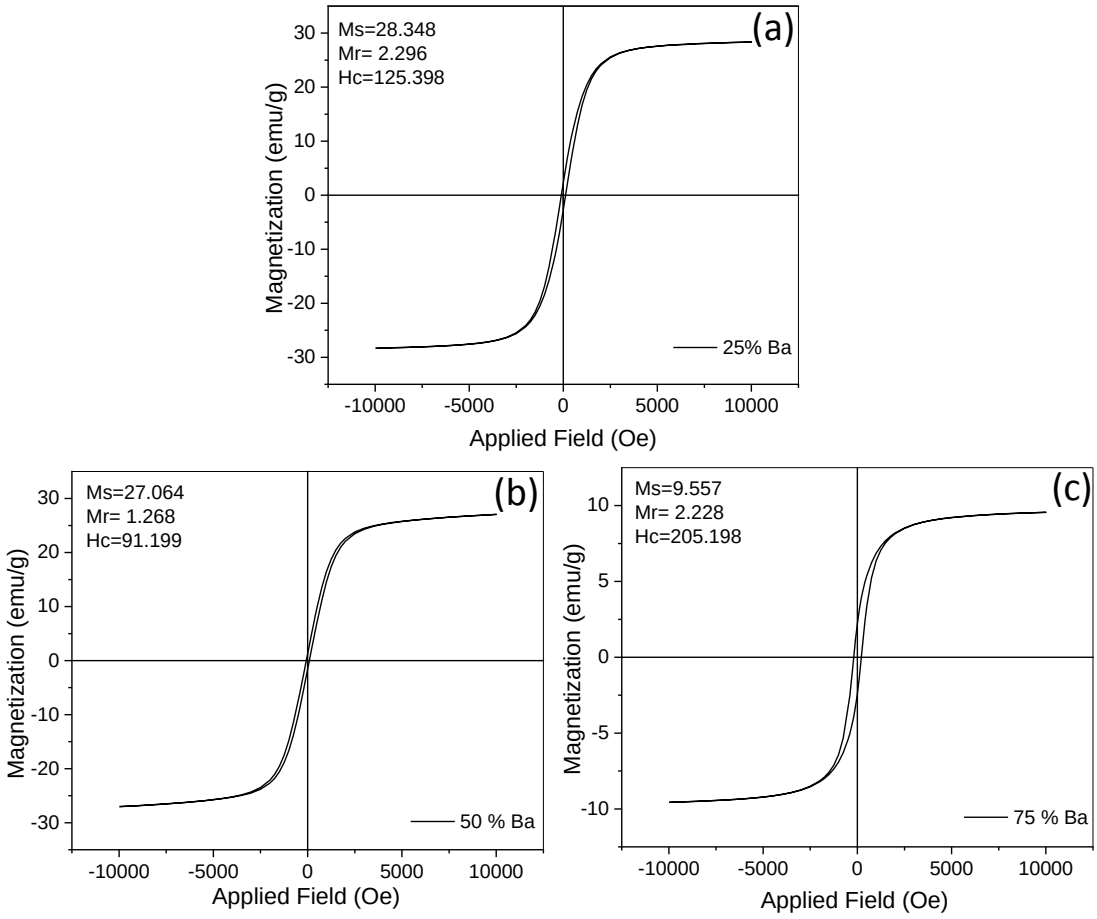

Figure 4-5 a- hysteresis loops soft(nickel) /hard(barium) with 25% Ba sintering at 1200°C b- hysteresis loops soft(nickel) /hard(barium) with 50% Ba sintering at 1200°C c- hysteresis loops soft(nickel) /hard(barium) with 75% Ba sintering at 1200°C

With a maximum applied field of 10,000 Oe at room temperature, VSM measurements were taken. A hysteresis loop was created for each measurement, and it was from this loop that the Calculations were made for intrinsic coercivity (Hc) and saturation magnetization (Ms).

In Figure (4.14) shown a hysteresis loop developed for the barium ferrite with a high coercively (Hc) . For pure M-type barium ferrite, the maximum coercivity is obtained due to the significant uniaxial anisotropy along the c-axis. association between Ms and Hc and discovered that it is dependent strongly on the cationic combination, and they came to the conclusion that this is unmistakably connected to the preference for the barium ferrite's Fe^{3+} sites being occupied , this will be agrees with a previous study, This agrees with Ref [120].

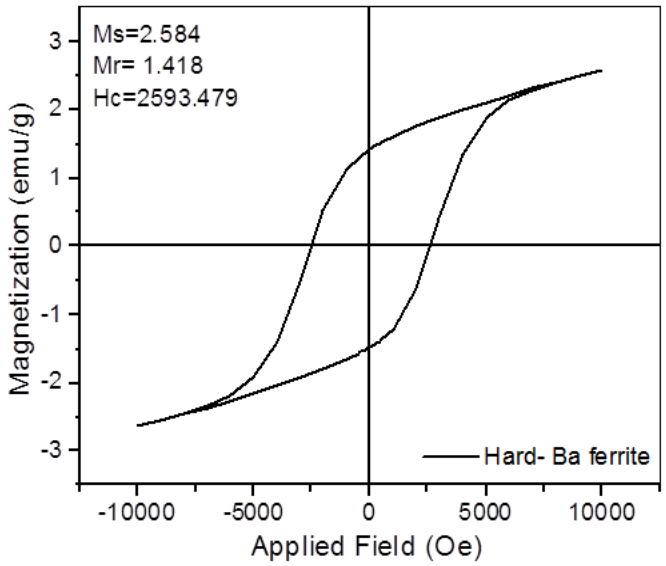

Figure 4-6 hysteresis loop developed for the barium ferrite .

Figure (4.15) depicted the magnetic saturation (MS), reminisce (Mr), and coercively (HC) of the soft/hard/soft layers in composites as being significantly

elevated. The composite nanoparticles showed single phase magnetization loop like that of a typical permanent magnet despite being made of two magnetically distinct phases, demonstrating that the two phases are exchanged coupled[123]. VSM data are illustrated in the table(4-2).

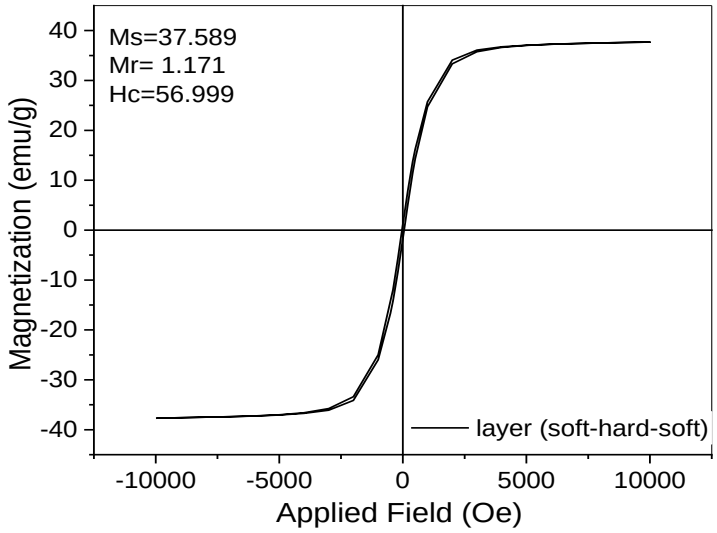

Figure 4-7 showed hysteresis loop developed for the layers soft/hard/soft ferrites

In a figure (4.16a,b ,c) show the different hysteresis loop of different ferrite samples , can be seen higher Ms for soft and layers samples , Hc the highest value for hard (barium ferrite) and for samples with a high barium ferrite ratio.

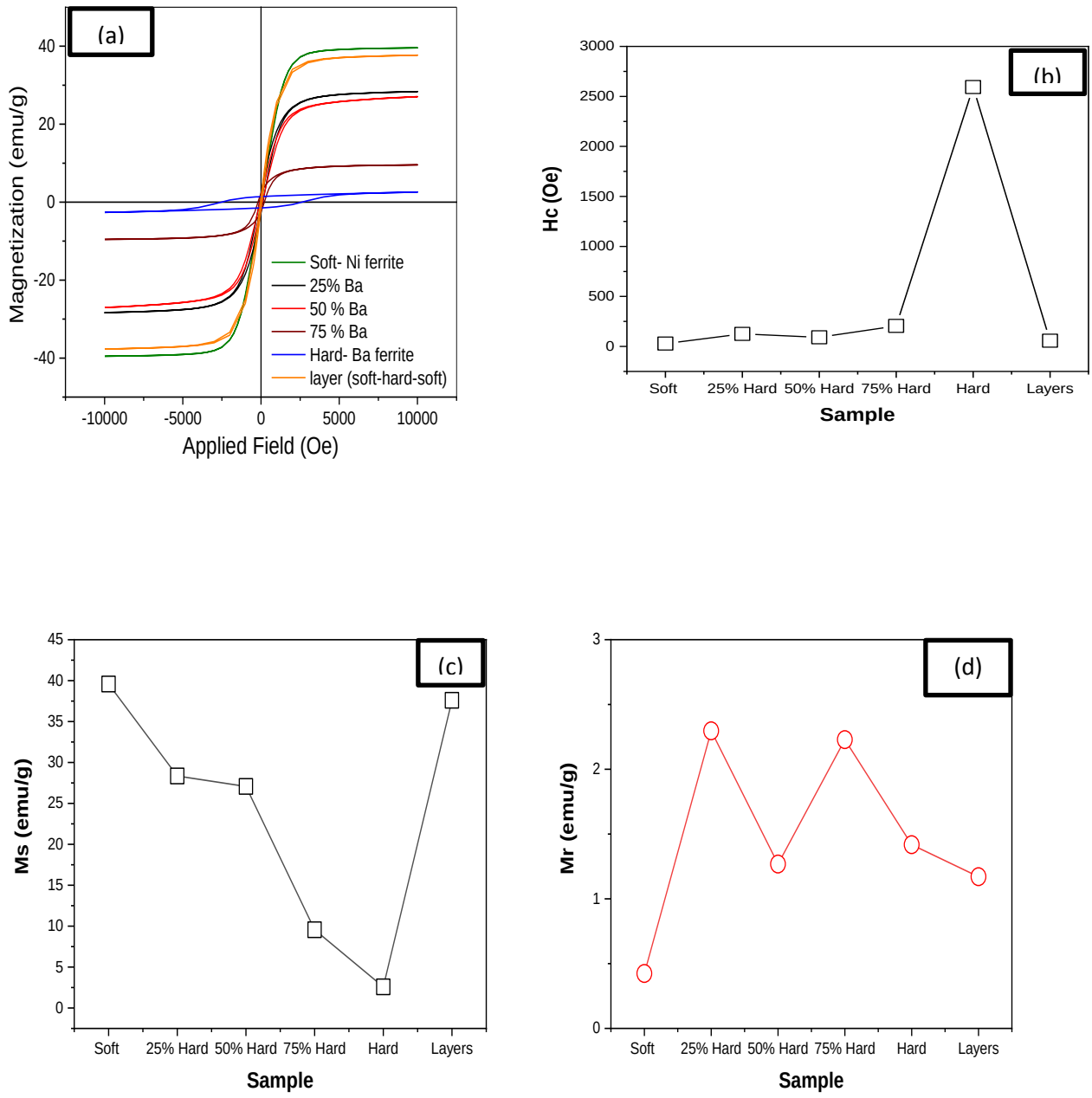

Figure 4-8 a- Hysteresis loops at 1200 °C temperature for nickel ferrite ,composite ferrite , barium ferrite and layers b- coricivity (Hc) for ferrite samples b,d- Ms, Mr for ferrite samples

Table 4-2 Magnetic properties of Ferrites Samples

Ferrites	Calcination temp.(°C)	Ms (emu/g)	Mr (emu/g)	Hc(Oe)	Mr /Ms
Nickel ferrite	1200°C	39.586	0.367	28.499	0.0092
Barium ferrite	1200°C	2.584	1.1418	2593.479	0.441
Composite ferrite with a ratio 25BF/75NF	1200°C	28.348	2.296	125.398	0.0809
Composite ferrite with ratio 50NF/50BF	1200°C	27.064	1.268	91.199	0.0468
Composite ferrite with a ratio 25NF/75BF	1200°C	9.557	2.228	205.198	0.2331
Layers	1200°C	37.589	1.171	56.999	0.0311

4.3 Physical Characterization of Ferrite

Table (4.3) shows the (apparent density, porosity, shrinkage) for different samples after pressing and sintering at 1200°C for pure composite and layered samples. apparent density of Barium ferrite and composite with higher ratio of barium ferrite is increase than the other nickel ferrite samples because of the

density of barium ferrite higher than nickel ferrite . The porosity of the samples, where we notice that the porosity of nickel ferrite is higher compared to other pressed and sintered samples under the same conditions and temperature. interesting to know that the increase of barium ferrite in the composite sample causes decrement in porosity value as shown in SEM figure (4-9).

The shrinkage of the samples, after calculating the dimensions of the compressed samples utilizing the digital vernier before and after the sintering process, a slight shrinkage in diameter was observed after sintering by 1200°C.

Table 4-3 Physical Characterization

Samples	Density g/cm^3	Porosity %	Shrinkage %
Nickel ferrite	1.5	50%	12.7%
Barium ferrite	2.3	10%	6.3%
Composite ferrite with ratio 50/50	3.5	60%	24.4%
Composite ferrite with a ratio 25BF/75NF	2.34	50%	12.6%
Composite ferrite with a ratio25NF/75BF	3.4	25%	7.6%
Layers	3.35	15%	14.5%

Chapter Five

5 Conclusion and Recommendation

5.1 Conclusion

1. The possibility of synthesized pure spinel $NiFe_2O_4$, $BaFe_2O_4$, composite and layers of nickel ferrite and barium ferrite by using sol gel process .Sol gel method , one of low-cost method to prepare ferrites nanopowder in a pure form and controlling the particle size through it.

2. XRD showed high purity of the nickel ferrite, barium ferrite nanoparticles at calcination temperature (600 °C,800°C) and sintering temperature (1200°C). where show in 600°C the main peak of nickel ferrite , at 800 °C show the peak of barium ferrite and the tow different peaks of barium and nickel ferrite depend on the ratio of nickel ferrite and barium ferrite.

3. In the FT-IR for nickel ferrite, two primary wide metal-oxygen bands are visible in the wavenumber region of 1000-400 cm-1, FT -IR spectrum of barium ferrite after sintering at 1200 °C, s characteristics broad peaks at 3354 cm-1 and for the nanocomposite hard/soft ferrites show absorption bands at 440 cm-1,541cm-1-,and 595cm-1.

4. The morphology of the Pure nickel ferrite, barium ferrite , nanocomposite ferrites and layers have been clarified the agglomeration of the spherical nanoparticles of nickel ferrite ,barium ferrite powder at 800°C SEM images exhibit a needle -like shape , For pressed sample after sintering at 1200°C incressing in particular size ,the SEM images of the composite material showed The observation of both nanoplatelets and quasispherical nanoparticles of spinel phase. For the layers the images show two types of layers, where the middle layer represents barium ferrite (hard ferrite) and the side layers represent nickel ferrite.

5. Physical properties were measured for pellet spinel NiFe2O4 , barium ferrite BaFe2O4 , nanocomposite and layers at 1200°C show the (apparent density, porosity, shrinkage) for different samples in table (4.2), density of Barium ferrite and composite with higher ratio of barium ferrite is higher than other samples , porosity in nickel ferrite is high and notes a little shrinkage occur in all ferrite samples.

6. The hysteresis loops of The Room Temp Ferromagnetism RTFM have different magnetization Ms , different hysteresis loops the S shape of soft nickel ferrite with a high magnetic saturation , high corctivity for a hard ferrite , single smooth hysteresis loop for a compo site and layers of hard/soft ferrites

5.2 Recommendation

1- Prepare ferrite by other methods, such as the chemical method, or studying synthesis the ferrite by using different substitution ions like Mn, Mg ions instead of Fe ion (divalent metal) or Al, Co ions as trivalent metal ions.
2- Prepared the ferrite layers with a different arrangement of the layers, like (hard ferrite – soft ferrite – hard ferrite) layers or with different numbers of layers.
3- Studying the multiferroic properties of ferrite nanoparticles, which interesting for solar light, sensors, actuators and memories applications.

6 References

1.Kakani, S. L. (2004). Material science. New Age International (P) Ltd., Publishers

2. Coey, J. M. D. (2002). Permanent magnet applications. Journal of Magnetism and Magnetic Materials, 248(3), 441-456

3. Nikmanesh, H., Moradi, M., Kameli, P., & Bordbar, G. H. (2017). Effects of annealing temperature on exchange spring behavior of barium hexaferrite/nickel zinc ferrite nanocomposites. Journal of Electronic Materials, 46, 5933-5941.

4. Kneller, E. F., & Hawig, R. (1991). The exchange-spring magnet: a new material principle for permanent magnets. IEEE Transactions on Magnetics, 27(4), 3588-3560

5. Nikmanesh, H., Moradi, M., Kameli, P., & Bordbar, G. H. (2017). Effects of annealing temperature on exchange spring behavior of barium hexaferrite/nickel zinc ferrite nanocomposites. Journal of Electronic Materials, 46(10), 5933-5941

6.Hoque, S. M., Srivastava, C., Kumar, V., Venkatesh, N., Das, H. N., Saha, D. K., & Chattopadhyay, K. (2013). Exchange-spring mechanism of soft and hard ferrite nanocomposites. Materials Research Bulletin, 48(8), 2871-2877

7. Hench, L. L., & West, J. K. (1990). Principles of Electronic Ceramics "John Wiley & Sons. New York.

8.A. B. Van Groenou, P. F. Bongers, A. L. Stuijts, Materials Science and Engineering, 3 (1968/69) 317.

9.Carl. Heck, in 1974 "Magnetic Materials and Their Applications" , Butterworths, London.

10.Cullity, B. D., & Graham, C. D. (2011). Introduction to magnetic materials. John Wiley & Sons

11. Sah, S. K. (2016). Magnetic Materials Characterization and Modeling for the Enhanced Design of Magnetic Shielding of Cryomodules in Particle Accelerators. Virginia Commonwealth University.

12.Hatch, G. P., Williams, A. J., & Harris, I. R. (1999). School of Metallurgy and Materials, University of Birmingham, Birmingham B15 2TT, UK. Advanced Hard and Soft Magnetic Materials: Volume 577, 577, 69

13. Chen C. 1986. Magnetism and metallurgy of soft magnetic materials. New York: Dover Publications.

14. Spaldin NA. 2003. Magnetic materials: fundamentals and device applications. Cambridge University.

15. Goldman, A. (2006). Modern ferrite technology. Springer Science & Business Media

16. M.A. Martens, R.J. Deissler, Y. Wu, L. Bauer, Z. Yao, R. Brown, et al. (2013), Modeling the Brownian relaxation of nanoparticle ferrofluids: comparison with experiment, Med. Phys. 40 (2) (2013) 022303.

17. Forrester, M., & Kusmartsev, F. (2014). The nano-mechanics and magnetic properties of high moment synthetic antiferromagnetic particles. physica status solidi (a), 211(4), 884-889.

18.Slimani, Y., Hannachi, E., Tombuloglu, H., Güner, S., Almessiere, M. A., Baykal, A., ... & Ercan, I. (2020). Magnetic nanoparticles based nanocontainers for biomedical application. In Smart Nanocontainers (pp. 229-250). Elsevier

19.Spaldin, Nicola A. (2011). Magnetic materials : fundamentals and applications (2nd ed.). Cambridge: Cambridge University Press. ISBN 978-0-521-88669-7. OCLC 607986416.

20. Chen C., 1986. "Magnetism and Metallurgy of Soft Magnetic Materials", Dover Publications, Inc., New York.

21. Richa Srivastava, and B. C. Yadav, 2012 " Ferrite Materials: Introduction, Synthesis Techniques, and Applications as Sensors", Taylor & Francis Group, LLC, International Journal of Green Nanotechnology, pp. 4:141–154.

22. Snoek J. L., 1977."New Developments in Ferromgnetic Materials", Elsevier Publishing Co., Inc., New York – Amsterdam, pp. 3-4.

23.Srivastava, R., & Yadav, B. C. (2012). Ferrite materials: introduction, synthesis techniques, and applications as sensors. International Journal of Green Nanotechnology, 4(2), 141-154

24.Kotnala, R. K., & Shah, J. (2015). Ferrite materials: nano to spintronics regime. In Handbook of magnetic materials (Vol. 23, pp. 291-379). Elsevier

25.Spaldin, Nicola A. (2010). Magnetic Materials: Fundamentals and Applications, 2nd Ed. Cambridge University Press. p. 120. ISBN 9781139491556.

26.Pullar, Robert C. (September 2012). "Hexagonal ferrites: A review of the synthesis, properties and applications of hexaferrite ceramics". Progress in Materials Science. 57 (7): 1191–1334. doi:10.1016/j.pmatsci.2012.04.001

27.Zate, M. K., Raut, S. D., Shirsat, S. D., Sangale, S., & Kadam, A. S. (2020). Ferrite nanostructures: Synthesis methods. In Spinel Ferrite Nanostructures for Energy Storage Devices (pp. 13-34). Elsevier

28. Okamoto, A. (2009). "The Invention of Ferrites and Their Contribution to the Miniaturization of Radios". 2009 IEEE Globecom Workshops. pp. 1–42. doi:10.1109/GLOCOMW.2009.5360693.ISBN 978-1-4244-5626-0.
S2CID 44319879.

29. Rawat, P. S., Srivastava, R. C., Dixit, G., Joshi, G. C., & Asokan, K. (2019, July). Facile synthesis and temperature dependent dielectric properties of MnFe2O4 nanoparticles. In AIP Conference Proceedings (Vol. 2115, No. 1, p. 030104). AIP Publishing LLC.

30. Ullah, Zaka; Atiq, Shahid; Naseem, Shahzad (2013). "Influence of Pb doping on structural, electrical and magnetic properties of Sr-hexaferrites". Journal of Alloys and Compounds. 555: 263–267.

31. " Gomes, J. D. A., Sousa, M. H., Tourinho, F. A., Aquino, R., da Silva, G. J., Depeyrot, J., ... & Perzynski, R. (2008). Synthesis of core− shell ferrite nanoparticles for ferrofluids: Chemical and magnetic analysis. The Journal of Physical Chemistry C, 112(16), 6220-6227

32.Gunjakar JL, More AM, Gurav KV, Lokhande CD. Chemical synthesis of spinel nickel ferrite (NiFe2O4) nano-sheets. Appl Surf Sci. 2008;254(18):5844–5848. doi: 10.1016/j.apsusc.2008.03.065.

33. Goldman A. 1993.Modern Ferrite Technology. New York: Marcel Dekker.

34. Alarifi A, Deraz NM, Shaban S. Structural, morphological and magnetic properties of NiFe2O4 nano-particles. J Alloys Compd. 2009;486(1-2):501–506. doi: 10.1016/j.jallcom.2009.06.192.

35. Manova E, Tsoncheva T, Paneva D, Mitov I, Tenchev K, Petrov L. Mechanochemically synthesized nano-dimensional iron-cobalt spinel oxides as

catalysts for methanol decomposition. Appl Catal A. 2004;277(1-2):119–127. doi: 10.1016/j.apcata.2004.09.002.

36. Baykal Al, Kasapoglu N, Koseoglu Yk, Toprak MS, Bayrakdar H. CTAB-assisted hydrothermal synthesis of NiFe2O4 and its magnetic characterization. J Alloys Compd. 2008;464(1-2):514–518. doi: 10.1016/j.jallcom.2007.10.041.

37. Ahlawat, A., Sathe, V. G., Reddy, V. R., & Gupta, A. (2011). Mossbauer, Raman and X-ray diffraction studies of superparamagnetic NiFe2O4 nanoparticles prepared by sol–gel auto-combustion method. Journal of Magnetism and Magnetic Materials, 323(15), 2049-2054

38. Bhuiyan MA, Hoque SM, Choudhury S. 2010. Effects of sintering temperature on microstructure and magnetic properties of NiFe2O4 prepared from nano size powder of NiO and Fe2O3, J Bangladesh Acad Sci. 2010;34(2):189–195.

39. "Ferrite Permanent Magnets". Arnold Magnetic Technologies. Archived from the original on 14 May 2012. Retrieved 18 January 2014. .

40. Erchak Jr, M., Fankuchen, I., & Ward, R. (1946). Reaction between ferric oxide and barium carbonate in the solid phase. Identification of phases by x-ray diffraction1. Journal of the American Chemical Society, 68(10), 2085-2093

41."Amorphous Magnetic Cores". Hill Technical Sales. 2006. Retrieved 18 January 2014.

42. Sembiring, T., Sasniati, P., Muljadi, Sinuhaji, P., & Sebayang, K. (2020, March). Study of physical and magnetic properties of barium hexaferrite substituted by Nd2O3. In AIP Conference Proceedings (Vol. 2221, No. 1, p. 110025).

43. J. Smith, H.P.J. 1959 . Wijin Ferrites, Wiley Philips TechnicalLibrary, 1959 pp. 177–178.

44. Trukhanov S.V., Trukhanov A.V., Turchenko V.O., Kostishyn V.G., Panina L.V., Kazakevich I.S., Balagurov A.M. Structure and Magnetic Properties of BaFe11.9In0.1O19 Hexaferrite in a Wide Temperature Range. J. Alloys Compd. 2016;689:383–393. doi: 10.1016/j.jallcom.2016.07.309.

45. Zhang H., Liu Z., Ma C., Yao X., Zhang L., Wu M. Complex Permittivity, Permeability, and Microwave Absorption of Zn- and Ti-Substituted Barium Ferrite by Citrate Sol–Gel Process. Mater. Sci. Eng. B. 2002;96:289–295.

46.Dimri, M. C., Khanduri, H., Agarwal, P., Pahapill, J., & Stern, R. (2019). Structural, magnetic, microwave permittivity and permeability studies of barium monoferrite (BaFe2O4). Journal of Magnetism and Magnetic Materials, 486, 165278.ISO 690

47. Yu, C., Sokolov, A. S., Kulik, P., & Harris, V. G. (2020). Stoichiometry, phase, and texture evolution in PLD-grown hexagonal barium ferrite films as a function of laser process parameters. Journal of Alloys and Compounds, 814, 152301

48. Barry C. Caster, and M. Grant Norton, 2007."Ceramic Materials Science and Engineering", Springer, 2007, pp. 612 -614

49.Hosni (2016). "Semi-hard magnetic properties of nanoparticles of cobalt ferrite synthesized by the co-precipitation process". Journal of Alloys and Compounds. 694: 1295–1301. doi:10.1016/j.jallcom.2016.09.252.

50. Olabi, A. G., & Grunwald, A. (2008). Design and application of magnetostrictive materials. Materials & Design, 29(2), 469-483.

ISO 690

51. Turtelli, R. S., Kriegisch, M., Atif, M., & Grössinger, R. (2014, June). Co-ferrite–A material with interesting magnetic properties. In IOP Conference Series: Materials Science and Engineering (Vol. 60, No. 1, p. 012020). IOP Publishing

52. Aubert, A., Loyau, V., Mazaleyrat, F., & Lobue, M. (2017). Enhancement of the magnetoelectric effect in multiferroic CoFe 2 O 4/PZT bilayer by induced uniaxial magnetic anisotropy. IEEE Transactions on Magnetics, 53(11), 1-5

53. Valenzuela, R. (1994). Magnetic ceramics (No. 4). Cambridge university press

54. Shinde, S. S. (2016). Crystal structure and magnetic interactions of ferrites. International Journal of Science and Research, 5, 1034

55. Tatarchuk, T., Bououdina, M., Judith Vijaya, J., & John Kennedy, L. (2016, August). Spinel ferrite nanoparticles: synthesis, crystal structure, properties, and perspective applications. In International conference on nanotechnology and nanomaterials (pp. 305-325). Springer, Cham

56. Pham, T. N., Huy, T. Q., & Le, A. T. (2020). Spinel ferrite (AFe 2 O 4)-based heterostructured designs for lithium-ion battery, environmental monitoring, and biomedical applications. RSC advances, 10(52), 31622-31661

57. Mastai, Y. (Ed.). (2012). Advances in crystallization processes. BoD–Books on Demand

58. Sickafus, Kurt E.; Wills, John M.; Grimes, Norman W. (2004-12-21). "Structure of Spinel". Journal of the American Ceramic Society. 82 (12): 3279–3292. doi:10.1111/j.1151-2916.1999.tb02241.x.

59. Carta, D., Casula, M. F., Falqui, A., Loche, D., Mountjoy, G., Sangregorio, C., & Corrias, A. (2009). A structural and magnetic investigation of the inversion

degree in ferrite nanocrystals MFe2O4 (M= Mn, Co, Ni). The Journal of Physical Chemistry C, 113(20), 8606-8615

60.Shahab Torkian, Ali Ghasemi , Reza Shoja Razavi, (2016) . Magnetic properties of hardsoft SrFe10Al2O19/Co0.8Ni0.2Fe2O4ferrite, synthesized by one-pot sol–gel autocombustion,mJ. Magn. Magn. Mater. 416 (2016) 408–416.

61. S. Tyagi, P. Verma, H. B. Baskey, R. C. Agarwala, V. Agarwala, T. C. Shami, (2012) .Microwave absorption study of carbon nano tubes dispersed hard/soft ferrite nanocomposite, Ceram. Int. 34 (2012) 4561–4571.

62. X. Q. Shen, F. Z. Song, J. Xiang, M. Q. Liu, Y. W. Zhu, Y. D. Wang, (2012) .ShapemAnisotropy, Exchange-Coupling Interaction and Microwave Absorption of Hard/Soft Nanocomposite Ferrite, J. Am. Ceram. Soc. 95 (2012) 3863–3870.

63. Kozlovskiy, A.L.; Zdorovets, M.V. 2020. The study of the structural characteristics and catalytic activity of Co/CoCo2O4 nanowires. Compos. Part B Eng. 2020, 191, 107968.

64. Kozlovskiy, A.L.; Kenzhina, I.E.; Zdorovets, M.V. 2020. FeCo–Fe2CoO4 /Co3O4 nanocomposites: Phase transformations as a result of thermal annealing and practical application in catalysis. Ceram. Int. 2020, 46, 10262–10269.

65. Pathania, A.; Thakur, P.; Trukhanov, A.V.; Trukhanov, S.V.; Panina, L.V.; Lüders, U.; Thakur, A.; Tomar, M.;Gupta, V. 2019. Development of tungsten doped Ni-Zn nano-ferrites with fast response and recovery time for hydrogen gas sensing application. Results Phys. 2019, 15, 102531.

66. Venturini, J.; Tonelli, A.M.; Wermuth, T.B.; Zampiva, R.Y.S.; Arcaro, S.; Da Cas Viegas, A.; Bergmann, C.P. 2020. Excess of cations in the sol-gel synthesis of cobalt ferrite (CoFe2O4): A pathway to switching the inversion degree of spinels.

J. Magn. Magn. Mater. 2019, 482, 1–8. [CrossRef] Nanomaterials 2020, 10, 2134 16 of 18

67. Dukenbayev, K.; Korolkov, I.V.; Tishkevich, D.I.; Kozlovskiy, A.L.; Trukhanov, S.V.; Gorin, Y.G.; Shumskaya, E.E.; Kaniukov, E.Y.; Vinnik, D.A.; Zdorovets, M.V.; et al. 2019. Fe3O4 Nanoparticles for Complex Targeted Delivery and Boron Neutron Capture Therapy. Nanomaterials 2019, 9, 494.

68. Meng, X.F.; Hana, Q.X.; Sun, Y.J.; Liu, Y.F. . 2019. Synthesis and microwave absorption properties of Ni0.5Zn0.5Fe2O4 /BaFe12O19@polyaniline composite. Ceram. Int. 2019, 45, 2504–2508.

69. Almessiere, M.A.; Trukhanov, A.V.; Slimani, Y.; You, K.Y.; Trukhanov, S.V.; Trukhanova, E.L.; Esa, F.; Sadaqat, A.; Chaudhary, K.; Zdorovets, M.; et al. 2019. Correlation between composition and electrodynamics properties in nanocomposites based on hard/soft ferrimagnetics with strong exchange coupling. Nanomaterials 2019, 9, 202.

70. Xu, Y.F.; Man, Y.Q.; Xu, S.T.; Zan, F.L.; Zheng, G.H.; Dai, Z.X. 2014. Obtainment of exchange coupling coefficient of Ni0.6Zn0.4Fe2O4 /SrFe12O19 composites. Mater. Lett. 2014, 131, 203–205.

71. Hazra, S., & Ghosh, N. N. (2014). Preparation of nanoferrites and their applications. Journal of nanoscience and nanotechnology, 14(2), 1983-2000

72. Laali, K. K., Greves, W. J., Correa-Smits, S. J., Zwarycz, A. T., Bunge, S. D., Borosky, G. L., ... & Chanan-Khan, A. (2018). Novel fluorinated curcuminoids and their pyrazole and isoxazole derivatives: Synthesis, structural studies, Computational/Docking and in-vitro bioassay. Journal of Fluorine Chemistry, 206, 82-98

73.Coldebella, E. H., Chagas, E. F., Albuquerque, A. P., Prado, R. J., Alzamora, M., & Baggio-Saitovitch, E. (2021). Study of soft/hard bimagnetic CoFe2/CoFe2O4 nanocomposite. Journal of Nanoscience and Nanotechnology, 21(10), 5181-5187

74. Goll, D., Seeger, M., & Kronmüller, H. (1998). Magnetic and microstructural properties of nanocrystalline exchange coupled PrFeB permanent magnets. Journal of Magnetism and Magnetic Materials, 185(1), 49-60.

75. Cha, H. G., Kim, Y. H., Kim, C. W., Kwon, H. W., & Kang, Y. S. (2007). Preparation for exchange-coupled permanent magnetic composite between α-Fe (soft) and Nd2Fe14B (hard). Current Applied Physics, 7(4), 400-403

76Schrefl, T., Kronmüller, H., & Fidler, J. (1993). Exchange hardening in nano-structured two-phase permanent magnets. Journal of magnetism and magnetic materials, 127(3), L273-L277.

77.Moon, K. W., Cho, S. G., Choa, Y. H., Kim, K. H., & Kim, J. (2007). Synthesis and magnetic properties of nano Ba-hexaferrite/NiZn ferrite composites. physica status solidi (a), 204(12), 4141-4144

78.Shaikh, S. F., Ubaidullah, M., Mane, R. S., & Al-Enizi, A. M. (2020). Types, synthesis methods and applications of ferrites. In Spinel Ferrite Nanostructures for Energy Storage Devices (pp. 51-82). Elsevier

79.Klein, L.C. and Garvey, G.J., (1980). "Kinetics of the Sol-Gel Transition" Journal of Non-Crystalline Solids, Vol. 38, p.45 (1980)

80. Brinker, C. J., Keefer, K. D., Schaefer, D. W., & Ashley, C. S. (1982). Sol-gel transition in simple silicates. Journal of Non-Crystalline Solids, 48(1), 47-64

81.Bokov, D., Turki Jalil, A., Chupradit, S., Suksatan, W., Javed Ansari, M., Shewael, I. H., ... & Kianfar, E. (2021). Nanomaterial by sol-gel method: synthesis and application. Advances in Materials Science and Engineering, 2021

82. Bokov, D., Turki Jalil, A., Chupradit, S., Suksatan, W., Javed Ansari, M., Shewael, I. H., ... & Kianfar, E. (2021). Nanomaterial by sol-gel method: synthesis and application. Advances in Materials Science and Engineering, 2021

83.M. Niederberger and N. Pinna, 2009. Metal Oxide Nanoparticles in Organic Solvents: Synthesis, Formation, Assembly and Application, Springer, NY, USA, 2009.

84.che R.X., Gao H., Zhao H.B., Fang J.X., Developing history and presentsituation of sol-gel science, 2005. Journal of Yunnan University, 2005, 27(3A), 378-383

85. Wang J., Li Ch., Xu B., 2009, Basic Principle, Advance and Current ApplicationSituation of Sol-Gel Method, CHEMICAL INDUSTRY AND ENGINEERING, 2009,26(3), 273-277

86. Brinker, C. J., & Scherer, G. W. (2013). Sol-gel science: the physics and chemistry of sol-gel processing. Academic press

87. Sakka, S. (2013). Sol–gel process and applications. Handbook of Advanced Ceramics, 2, 883-910.

88. Teh, G. B., Nagalingam, S., & Jefferson, D. A. (2007). Preparation and studies of Co (II) and Co (III)-substituted barium ferrite prepared by sol–gel method. Materials Chemistry and Physics, 101(1), 158-162

89. Paimozd, E., Ghasemi, A., Jafari, A., & Sheikh, H. (2008). Influence of acid catalysts on the structural and magnetic properties of nanocrystalline barium ferrite

prepared by sol–gel method. Journal of magnetism and magnetic materials, 320(23), L137-L140

90. Rai, B. K., Wang, L., Mishra, S. R., Nguyen, V. V., & Liu, J. P. (2014). Synthesis and magnetic properties of hard-soft SrFe10Al2O19/NiZnFe2O4 ferrite nanocomposites. Journal of Nanoscience and Nanotechnology, 14(7), 5272-5277

91. Neupane, D., Ghimire, M., Adhikari, H., Lisfi, A., & Mishra, S. R. (2017). Synthesis and magnetic study of magnetically hard-soft SrFe12-yAlyO19-x Wt.% Ni0. 5Zn0. 5Fe2O4 nanocomposites. AIP Advances, 7(5), 055602

92. Khan, A. A., Javed, M., Khan, A. R., Iqbal, Y., Majeed, A., Hussain, S. Z., & Durrani, A. S. (2017). Influence of preparation method on structural, optical and magnetic properties of nickel ferrite nanoparticles. Materials Science-Poland, 35(1), 58-65

93. Tavakolinia, F., Yousefi, M., Afghahi, S. S. S., Baghshahi, S., & Samadi, S. (2018). Synthesis of novel hard/soft ferrite composites particles with improved magnetic properties and exchange coupling. Processing and Application of Ceramics, 12(3), 248-256

94. Peymanfar, R., Rahmanisaghieh, M., Ghaffari, A., & Yassi, Y. (2018). Preparation and Identification of BaFe2O4 Nanoparticles by the Sol–Gel Route and Investigation of Its Microwave Absorption Characteristics at Ku-Band Frequency Using Silicone Rubber Medium. Multidisciplinary Digital Publishing Institute Proceedings, 2(17), 5234

95. Hussain, S. A. (2019, July). Investigation of the Structure and Magnetic Properties of Co+ 2–Ti+ 4 Substituted Barium Ferrite Powder Prepared by Sol–Gel Method. In Journal of Physics: Conference Series (Vol. 1234, No. 1, p. 012052). IOP Publishing

96. Kahnes, M., & Töpfer, J. (2019). Synthesis and magnetic properties of hard/soft SrAl2Fe10O19/Fe (FeCo2) nanocomposites. Journal of Magnetism and Magnetic Materials, 480, 40-46

97. Algarou, N. A., Slimani, Y., Almessiere, M. A., Baykal, A., Guner, S., Manikandan, A., & Ercan, I. (2020). Enhancement on the exchange coupling behavior of SrCo0. 02Zr0. 02Fe11. 96O19/MFe2O4 (M= Co, Ni, Cu, Mn and Zn) as hard/soft magnetic nanocomposites. Journal of Magnetism and Magnetic Materials, 499, 166308

98. Lee, J., Lee, G., Hwang, T. Y., Lim, H. R., Cho, H. B., Kim, J., & Choa, Y. H. (2020). Phase-and Composition-Tunable Hard/Soft Magnetic Nanofibers for High-Performance Permanent Magnet. ACS Applied Nano Materials, 3(4), 3244-3251

99. Irfan, H., & Vizhi, R. E. (2020). Enhancement of the maximum energy product in Ba0. 5Sr0. 5Fe12O19/Y3Fe5O12 nanocomposites synthesized by the co-precipitation method. Nanotechnology, 31(40), 404001

100. Almessiere, M. A., Slimani, Y., Attia, H., Sheikh, S. I. M., Sadaqat, A., Vakhitov, M. G., ... & Trukhanov, A. V. (2021). Alterations in the magnetic and electrodynamic properties of hard-soft Sr0. 5Ba0. 5Eu0. 01Fe12O19/NixCuyZnwFe2O4 nanocomposites. Journal of Materials Research and Technology, 15, 1416-1429

101. Almessiere, M. A., Slimani, Y., Trukhanov, A. V., Sadaqat, A., Korkmaz, A. D., Algarou, N. A., ... & Toprak, M. S. (2021). Review on functional bi-component nanocomposites based on hard/soft ferrites: structural, magnetic, electrical and microwave absorption properties. Nano-Structures & Nano-Objects, 26, 100728

102. Slimani, Y., Algarou, N. A., Almessiere, M. A., Sadaqat, A., Vakhitov, M. G., Klygach, D. S., ... & Ercan, I. (2021). Fabrication of exchange coupled hard/soft magnetic nanocomposites: Correlation between composition, magnetic, optical and microwave properties. Arabian Journal of Chemistry, 14(3), 102992

103. Mitchell, B. S. (2004). An introduction to materials engineering and science for chemical and materials engineers. John Wiley & Sons

104. Ansari, A., Ali, A., & Asif, M. (2018). Microwave-assisted MgO NP catalyzed one-pot multicomponent synthesis of polysubstituted steroidal pyridines. New Journal of Chemistry, 42(1), 184-197

105. Caddy, B. (Ed.). (2002). Forensic examination of glass and paint: analysis and interpretation. CRC Press

106. Torres-Rivero, K., Bastos-Arrieta, J., Fiol, N., & Florido, A. (2021). Metal and metal oxide nanoparticles: An integrated perspective of the green synthesis methods by natural products and waste valorization: applications and challenges. Comprehensive Analytical Chemistry, 94, 433-469

107.Pradeep, A., Priyadharsini, P., & Chandrasekaran, G. (2008). Sol gel route of synthesis of nanoparticles of MgFe2O4 and XRD, FTIR and VSM study. Journal of Magnetism and Magnetic Materials, 320 (21), 2774-2779

108.Ghanbari, D., Sharifi, S., Naraghi, A., & Nabiyouni, G. (2016). Photo-degradation of azo-dyes by applicable magnetic zeolite Y-Silver–CoFe2O4 nanocomposites. Journal of Materials Science: Materials in Electronics , 27 (5), 5315 -5323

109.Standard, A. S. T. M. (2006). Standard Test Method for Water Absorption, Bulk Density, Apparent Porosity and Apparent Specific Gravity for Fired Whitewater Products. Annual Book ASTM Standard, 15, 112-113.

110. Hassan, M. A., Saqib, M., Shaikh, H., Ahmad, N. M., & Elaissari, A. (2013). Magnetically engineered smart thin films: toward lab-on-chip ultra-sensitive molecular imaging. Journal of biomedical nanotechnology, 9(3), 467-474

111. Nikmanesh, H., Moradi, M., Kameli, P., & Bordbar, G. H. (2017). Effects of annealing temperature on exchange spring behavior of barium hexaferrite/nickel zinc ferrite nanocomposites. Journal of Electronic Materials, 46(10), 5933-5941

112. Rashad, M. M., & Ibrahim, I. A. (2011). A novel approach for synthesis of M-type hexaferrites nanopowders via the co-precipitation method. Journal of Materials Science: Materials in Electronics, 22, 1796-1803

113. Dilip, R., Jayaprakash, R., Sangaiya, P., & Gopi, S. (2020). The magnetic property alterations due to transition from barium ferrite (BaFe2O4) nano rods to barium carbonate (BaCO3) quantum dots. Results in Materials, 7, 100121

114. Sivakumar, P., Ramesh, R., Ramanand, A., Ponnusamy, S., & Muthamizhchelvan, C. (2011). Synthesis and characterization of nickel ferrite magnetic nanoparticles. Materials Research Bulletin, 46(12), 2208-2211

115. Sharifi, F., Hedayati, K., & Ghanbari, D. (2022). Simple preparation and investigation of magnetic nanocomposites: Electrodeposition of polymeric aniline-barium ferrite and aniline-strontium ferrite thin films. Main Group Metal Chemistry, 45(1), 169-177

116. Jacob, B. P., Kumar, A., Pant, R. P., Singh, S., & Mohammed, E. M. (2011). Influence of preparation method on structural and magnetic properties of nickel ferrite nanoparticles. Bulletin of Materials Science, 34(7), 1345-1350

117. Ashiq, M. N., Ehsan, M. F., Iqbal, M. J., & Gul, I. H. (2011). Synthesis, structural and electrical characterization of Sb3+ substituted spinel nickel ferrite (NiSbxFe2− xO4) nanoparticles by reverse micelle technique. Journal of Alloys and Compounds, 509(16), 5119-5126

118. Yokoyama, M., Ohta, E., Sato, T., & Komaba, T. (1997). Size dependent magnetic properties of zinc ferrite fine particles. Le Journal de Physique IV, 7(C1), C1-521.

119.Xiang Jun, Shen Xiang-Qian, Song Fu-Zhan, and Liu Ming-Quan," 2009. Fabrication and magnetic properties of Ni0.5Zn0.5Fe2O4 nanofibers by electrospinning", Chin. Phys.Soc. and IOP Publishing Ltd, Vol18 No 11, November 2009

120. Dilip, R., Ravikumar, K., Chandekar, K. V., Shkir, M., Krishnan, V. G., Shinde, K. S., & Ashraf, I. M. (2022). Enhancement of magnetic and dielectrics performance of BaFe2O4 nanoparticles influenced by tri-sodium citrate as surfactant. Journal of Materials Science: Materials in Electronics, 33(30), 23841-23850

121. Primc, D., & Makovec, D. (2015). Composite nanoplatelets combining soft-magnetic iron oxide with hard-magnetic barium hexaferrite. Nanoscale, 7(6), 2688-2697

الخلاصة:

نظرا لتكوينها ,يشار أحيانا الى مغناطيس السيراميك بـاسم مغناطيس الفرايت . حيث تتكون من عده عناصر معدنيه وأكسد الحديد . تتحد هذه المواد لتكوين المركب المغناطيسي المعروف باسم الفرايت. مغناطيس الفرايت الصلب(Hard Ferrite)لديه قوة قسريه عاليه و مغناطيس الفرايت الناعم(Soft Ferrite)لديه قسر منخفض. مغناطيس الفرايت الناعم ذو القسر المنخفض عند تعرضه لمجال مغناطيسي خارجي من المرجح أن يفقد مغناطيسيته.

في هذا العمل تم تحضير ماده مركبه المتمثله الفرايت الصلب(Hard Ferrite)\اللين(Soft ferrite) وطبقات المتمثله ب طبقه لينه(Soft Layer)\طبقه صلبه(Haed Layer)\طبقه لينه(Soft Layer)

النيكل الفريت الإسبنيل (NiFe2O4) هو واحد من أكثر أنواع الفريت الناعمة شهرة ، وقد تم تصنيع كل من الفريت الصلب ذو الشكل الابري (الباريوم فرايت) ذو الخصائص الخاصة بطريقة sol-gel باستخدام نترات النيكل المائي ، نترات الباريوم ، نترات الحديد المائيه و الاثلين كلايكول كمواد اوليه ، بعد تحضير المسحوق تم حرقه لمدة خمس ساعات بمعدل 5 درجات مئوية / دقيقة حيث تم حرق النيكل فرايت عند 600 درجة مئوية و 800 درجة مئوية للفريت الباريوم من اجل الحصول عليه كمسحوق جاف. يمكن ان يقسم العمل الحالي الى جزأين رئيسيين، الجزء الأول هو تحضير مساحيق من الفيرايت اللين (نيكل فيرايت) والفيرايت صلب (باريوم فيرايت) ومركبهما بنسب مختلفة، ويتضمن الجزء الثاني تحضير الجسم المكبوس كفرايت نقي وفيرايت مركب أو على شكل طبقات بين الفيرايت اللين والصلب وتلبيده عند 1200 درجة مئوية. تم إجراء اختبار XRD وقد أظهرت النتائج الحصول على اطوار نقية للمساحيق فيرايتية النقية والمركبة من الفيرايت اللين والصلب حيث اظهرت القمم الرئيسية للنيكل فيرايت($NiFe_2O_4$) , الباريوم فيرايت بطوريه المختلفين عند درجات حراره مختلفة وكذلك القمم لمادتي النيكل والباريوم فيرايت لمركبهما اعتمادا على نسبه كل منهما, من خلال تحليل الطيف FTIR وجود الاواصر الأساسية للفيرايت النقي او الفيرايت المركب بين الروابط الرئيسية للنيكل فيرايت اعلى واحده المتمثلة ب V1عند المدى 550-630 cm^{-1} والرابطة الاقل المتمثلة ب v2 عند المدى cm^{-1}450-390 والباريوم فيرايت الروابط الرئيسية تتمثل عند ,1147cm-1,1058cm-1,1001cm-1وبالنسبة للفيرايت المركب تقع الترددات الرئيسية للروابط بين 570و1-cm 610، كما ان صور اختبار SEM أظهرت الجسيمات النانوية من نيكل فيرايت ذات الشكل

الكروي وتحتوي على مسامات بينما تظهر صور الفيرايت الباريوم الشكل السداسي وقد تم اجراء هذه الاختبارات قبل التلبيد وبعده.

ومن اجل دراسة الخواص المغناطيسية للفيرايت المحضر تم اجراء اختبار VSM يظهر قيم مغناطيسية مختلفة MS ، وحلقات هسترة مختلفة حيث يظهر شكل S من الفيرايت النيكل اللين مع تشبع مغناطيسي عالٍ ، وقوة قسرية عالية للفيرايت الصلب ، وحلقة هسترة واحدة لينة للفيرايت النانوي ذو الطبقات الفيرايت (اللين/ الصلب / اللين).تم اجراء هذا الاختبار بعد عمليه التلبيد .حيث وجدت اعلى قيمه للMs في الفيرايت اللين (39.586) وعند الطبقات (37.589) و اعلى قيمه للHc وجدت عند الفيرايت الصلب و العينة التي تكون فيها نسبه الباريوم فيرايت 75%.حيث الزيادة ب القوة القسرية و التشبع المغناطيسي يعتمد على نسبه الفيرايت الصلب و اللين.

وأخيرا تم اجراء مجموعة من الاختبارات الفيزيائية على الفيرايت المحضر وهي الكثافة والمسامية والانكماش وذلك بعد التلبيد عند 1200 درجة مئوية من اجل تحديد المواصفات الفيزيائية للمساحيق ,حيث ظهرت مسامات في العينات الملبده وحصول القليل من الانكماش في ابعاد العينات بعد اجراء عمليه التلبيد.

جمهورية العراق
وزارة التعليم العالي والبحث العلمي
جامعة بابل
كلية هندسة المواد
قسم هندسة السيراميك و مواد البناء

السلوك المغناطيسي لنظام نيكل فرايت/باريوم فرايت

رسالة
مقدمة إلى قسم السيراميك ومواد البناء في كلية هندسة المواد/جامعة بابل كجزء من متطلبات نيل درجة الماجستير في هندسة المواد/ السيراميك

من قبل

أماني حاتم شاكر مهدي

بأشراف

أ.م.د.شيماء جابر كريم
م.د محمد ناجي الأعرجي

1443 هـ
2023 م